

Hunting for primordial non-Gaussianity in the cosmic microwave background

Eiichiro Komatsu

Texas Cosmology Center and Department of Astronomy, The University of Texas at Austin, Austin, TX 78712, USA

E-mail: komatsu@astro.as.utexas.edu

Abstract. Since the first limit on the (local) primordial non-Gaussianity parameter, f_{NL} , was obtained from the *Cosmic Background Explorer (COBE)* data in 2002, observations of the cosmic microwave background (CMB) have been playing a central role in constraining the amplitudes of various forms of non-Gaussianity in primordial fluctuations. The current 68% limit from the 7-year data of the *Wilkinson Microwave Anisotropy Probe (WMAP)* is $f_{\text{NL}} = 32 \pm 21$, and the *Planck* satellite is expected to reduce the uncertainty by a factor of four in a few years from now. If $f_{\text{NL}} \gg 1$ is found by *Planck* with high statistical significance, all single-field models of inflation would be ruled out. Moreover, if the *Planck* satellite finds $f_{\text{NL}} \sim 30$, then it would be able to test a broad class of multi-field models using the four-point function (trispectrum) test of $\tau_{\text{NL}} \geq (6f_{\text{NL}}/5)^2$. In this article, we review the methods (optimal estimator), results (WMAP 7-year), and challenges (secondary anisotropy, second-order effect, and foreground) of measuring primordial non-Gaussianity from the CMB data, present a science case for the trispectrum, and conclude with future prospects.

1. Introduction

The physics of the very early, primordial universe is best probed by measurements of statistical properties of primordial fluctuations. The primordial fluctuations are the seeds for the temperature and polarization anisotropies of the CMB and the large-scale structure of the universe that we observe today. Therefore, both the CMB and the large-scale structure are excellent probes of the primordial fluctuations. In this article, we shall focus on the CMB. See the article by V. Desjacques and U. Seljak in this volume for the corresponding review on the large-scale structure as a probe of the primordial fluctuations.

This article reviews a recent progress on our using the CMB as a probe of a particular statistical aspect of primordial fluctuations called “*non-Gaussianity*.” Reviews on this subject were written in 2001 [1] and 2004 [2]. The former review would be most useful for those who are new to this subject.

In this article, we focus on the new discoveries that have been made since 2004. Particularly notable ones include:

1. It has been proven that *all* inflation models (not just simple ones [3, 4]) based upon a single scalar field would be ruled out regardless of the details of models [5], if the primordial non-Gaussianity parameter called f_{NL} (more precisely, the “local type” f_{NL} as described later) is found to be much greater than unity.
2. The optimal method for extracting f_{NL} from the CMB data has been developed [6–9] and implemented [10]. The latest limit on the local-type f_{NL} from the *WMAP* 7-year temperature data is $f_{\text{NL}} = 32 \pm 21$ (68% CL) [11].
3. The most serious contamination of the local-type f_{NL} due to the secondary CMB anisotropy, the coupling between the Integrated Sachs-Wolfe (ISW) effect and the weak gravitational lensing, has been identified [8, 12–16]. However, note that the astrophysical contamination such as the Galactic foreground emission and radio point sources may still be the most serious contaminant of f_{NL} . These effects would pose a serious analysis challenge to measuring f_{NL} from the *Planck* data.
4. The importance of distinguishing different triangle configurations of the three-point function of the CMB was realized [17, 18] and has been fully appreciated. It has been shown by many researchers that different configurations probe distinctly different aspects of the physics of the primordial universe. The list of possibilities is long, and a terribly incomplete list of references on recent work (since ~ 2004) is: [19] on a general analysis of various shapes; [20–25] on the local shape ($k_3 \ll k_1 \approx k_2$); [17, 26–28] on the equilateral shape ($k_1 \approx k_2 \approx k_3$); [29, 30] on the flattend (or folded) shape ($k_1 \approx 2k_2 \approx 2k_3$); [31] on the orthogonal shape (which is nearly orthogonal to both local and equilateral shapes); [32–36] on combinations of different shapes; and [37, 38] on oscillating bispectra. Also see references therein.
5. The connected four-point function of primordial fluctuations has been shown to be an equally powerful probe of the physics of the primordial universe. In particular, a combination of the three- and four-point functions may allow us to further distinguish different scenarios. Many papers have been written on this subject over the last few years: [39–42] on single-field models; [34, 43–63] on multi-field models; and [64, 65] on isocurvature perturbations. CMB data are expected to provide useful limits on the parameters of the “local-form trispectrum,” τ_{NL} and g_{NL} [66, 67]. Preliminary limits on these parameters have been obtained from the *WMAP* data by [68, 69].

The number of researchers working on primordial non-Gaussianity has increased dramatically: Science White Paper on non-Gaussianity submitted to Decadal Survey Astro2010 was co-signed by 61 scientists [70].

2. Gaussian versus non-Gaussian CMB anisotropy

2.1. What do we mean by “Gaussianity”?

What do we mean by “Gaussian fluctuations”? Let us consider the distribution of temperature anisotropy of the CMB that we observe on the sky, $\Delta T(\hat{\mathbf{n}})$. The

temperature anisotropy is Gaussian when its probability density function (PDF) is given by

$$P(\Delta T) = \frac{1}{(2\pi)^{N_{\text{pix}}/2} |\xi|^{1/2}} \exp \left[-\frac{1}{2} \sum_{ij} \Delta T_i (\xi^{-1})_{ij} \Delta T_j \right], \quad (1)$$

where $\Delta T_i \equiv \Delta T(\hat{\mathbf{n}})$, $\xi_{ij} \equiv \langle \Delta T_i \Delta T_j \rangle$ is the covariance matrix (or the two-point correlation function) of the temperature anisotropy, $|\xi|$ is the determinant of the covariance matrix, and N_{pix} is the number of pixels on the sky.

We often work in harmonic space by expanding ΔT using spherical harmonics: $\Delta T(\hat{\mathbf{n}}) = \sum_{lm} a_{lm} Y_{lm}(\hat{\mathbf{n}})$. The PDF for a_{lm} is given by

$$P(a) = \frac{1}{(2\pi)^{N_{\text{harm}}/2} |C|^{1/2}} \exp \left[-\frac{1}{2} \sum_{lm} \sum_{l'm'} a_{lm}^* (C^{-1})_{lm, l'm'} a_{l'm'} \right], \quad (2)$$

where $C_{lm, l'm'} \equiv \langle a_{lm}^* a_{l'm'} \rangle$, and N_{harm} is the number of l and m . When a_{lm} is statistically homogeneous and isotropic (which is not always the case because of, e.g., non-uniform noise), one finds $C_{lm, l'm'} = C_l \delta_{ll'} \delta_{mm'}$, and thus the PDF simplifies to

$$P(a) = \prod_{lm} \frac{e^{-|a_{lm}|^2/(2C_l)}}{\sqrt{2\pi C_l}}. \quad (3)$$

Here, C_l is the *angular power spectrum*. The latest determination of C_l of the CMB temperature anisotropy is shown in Figure 1.

The important property of a Gaussian distribution is that the PDF is fully specified by the covariance matrix. In other words, the covariance matrix contains all the information on statistical properties of Gaussian fluctuations. When the PDF is given by equation 3, the power spectrum, C_l , contains all the information on a_{lm} . This is not true for non-Gaussian fluctuations, for which one needs information on higher-order correlation functions.

Let us close this subsection by noting that a non-zero deviation of the covariance matrix from the diagonal form, $\Delta C_{lm, l'm'} = C_{lm, l'm'} - C_l \delta_{ll'} \delta_{mm'}$, does not imply non-Gaussianity: the PDF can be a Gaussian with a non-diagonal covariance matrix as given in equation 2. A non-zero $\Delta C_{lm, l'm'}$ may arise in cosmological models that violate statistical isotropy. Such models may yield *anisotropic Gaussian* fluctuations; thus, one must distinguish between non-Gaussianity and a violation of statistical isotropy.

2.2. What do we mean by “non-Gaussianity”?

What do we mean by “non-Gaussian fluctuations”? Any deviation from a Gaussian distribution (such as equation 1 or 2) is called *non-Gaussianity*. When fluctuations in the CMB are non-Gaussian, one cannot generally write down its PDF, unless one considers certain models (e.g., inflation). Nevertheless, when non-Gaussianity is weak, one may expand the PDF around a Gaussian distribution [74] and obtain

$$P(a) = \left[1 - \sum_{\text{all } l_i m_j} \langle a_{l_1 m_1} a_{l_2 m_2} a_{l_3 m_3} \rangle \frac{\partial}{\partial a_{l_1 m_1}} \frac{\partial}{\partial a_{l_2 m_2}} \frac{\partial}{\partial a_{l_3 m_3}} \right]$$

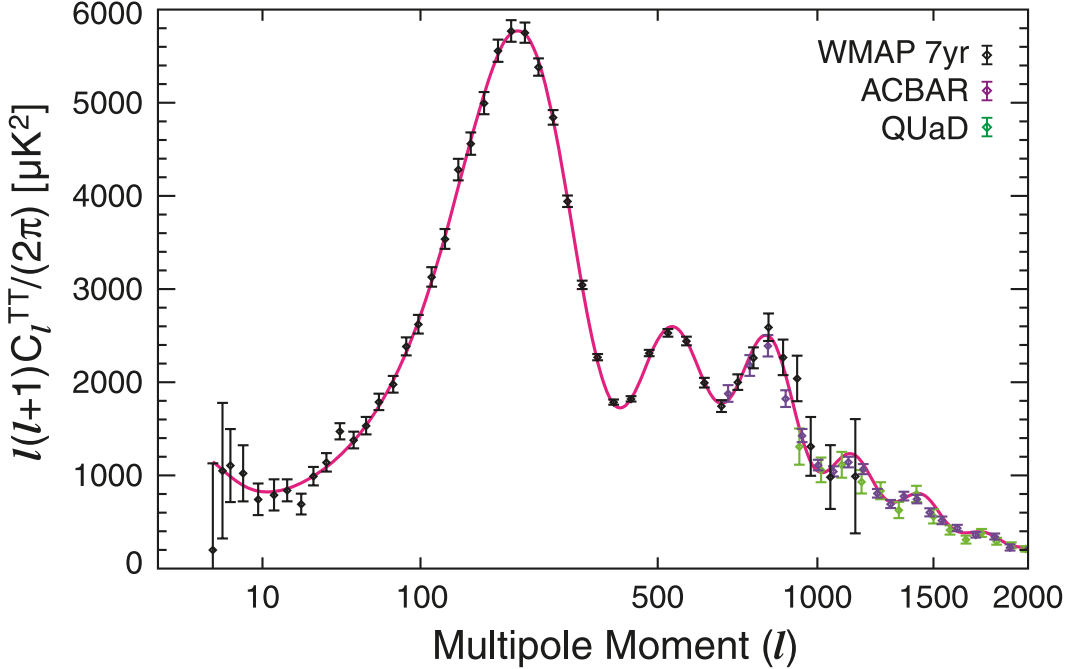


Figure 1. The angular power spectrum of the CMB temperature anisotropy, C_l , measured from the WMAP 7-year data [71], along with the temperature power spectra from the ACBAR [72] and QUaD [73] experiments. The solid line shows the best-fitting 6-parameter flat Λ CDM model to the WMAP data alone. The angular power spectrum contains all the information on fluctuations in the CMB, if fluctuations are Gaussian. If fluctuations are non-Gaussian, one must use the higher-order correlation functions (such as three- and four-point functions) to fully exploit the cosmological information contained in the CMB. This figure is adopted from [11].

$$\times \frac{e^{-\frac{1}{2} \sum_{lm} \sum_{l'm'} a_{lm}^* (C^{-1})_{lm, l'm'} a_{l'm'}}}{(2\pi)^{N_{\text{harm}}/2} |C|^{1/2}}. \quad (4)$$

Here, the expansion is truncated at the three-point function (bispectrum) of a_{lm} , and thus we have assumed that the connected four-point and higher-order correlation functions are negligible compared to the power spectrum and bispectrum. (This condition is not always satisfied.) By evaluating the above derivatives, one obtains[‡]

$$\begin{aligned} P(a) = & \frac{1}{(2\pi)^{N_{\text{harm}}/2} |C|^{1/2}} \exp \left[-\frac{1}{2} \sum_{lm} \sum_{l'm'} a_{lm}^* (C^{-1})_{lm, l'm'} a_{l'm'} \right] \\ & \times \left\{ 1 + \sum_{\text{all } l_i m_j} \langle a_{l_1 m_1} a_{l_2 m_2} a_{l_3 m_3} \rangle \left[(C^{-1} a)_{l_1 m_1} (C^{-1} a)_{l_2 m_2} (C^{-1} a)_{l_3 m_3} \right. \right. \\ & \left. \left. - 3(C^{-1})_{l_1 m_1, l_2 m_2} (C^{-1} a)_{l_3 m_3} \right] \right\}. \end{aligned} \quad (5)$$

This formula is useful, as it tells us how to estimate the *angular bispectrum*, $\langle a_{l_1 m_1} a_{l_2 m_2} a_{l_3 m_3} \rangle$, optimally from a given data by maximizing this PDF. In practice, we parametrize the bispectrum using a few parameters (e.g., f_{NL}), and estimate those parameters from the data by maximizing the PDF with respect to the parameters.

[‡] Babich [75] derived this formula for $C_{lm, l'm'} = C_l \delta_{ll'} \delta_{mm'}$.

In the limit that the contribution of the connected four-point function (trispectrum) to the PDF is negligible compared to those of the power spectrum and bispectrum, equation 5 contains all the information on non-Gaussian fluctuations characterized by the covariance matrix, $C_{l_1 m_1, l_2 m_2} = \langle a_{l_1 m_1}^* a_{l_2 m_2} \rangle$, and the angular bispectrum, $\langle a_{l_1 m_1} a_{l_2 m_2} a_{l_3 m_3} \rangle$. This approach can be extended straightforwardly to the trispectrum if necessary.

3. Extracting f_{NL} from the CMB data

3.1. General formula

We have not defined what we mean by “ f_{NL} .” For the moment, let us loosely define it as the *amplitude* of a certain shape of the angular bispectrum:

$$\langle a_{l_1 m_1} a_{l_2 m_2} a_{l_3 m_3} \rangle = \mathcal{G}_{l_1 l_2 l_3}^{m_1 m_2 m_3} \sum_i f_{\text{NL}}^{(i)} b_{l_1 l_2 l_3}^{(i)}, \quad (6)$$

where the function, $b_{l_1 l_2 l_3}^{(i)}$, is called the “reduced angular bispectrum” [76] and defines the shape of the angular bispectrum for a given model denoted by an index i (which may refer to, e.g., “local,” “equilateral,” “orthogonal,” etc), and $\mathcal{G}_{l_1 l_2 l_3}^{m_1 m_2 m_3}$ is the so-called Gaunt integral, defined by

$$\mathcal{G}_{l_1 l_2 l_3}^{m_1 m_2 m_3} \equiv \int d^2 \hat{\mathbf{n}} Y_{l_1 m_1}(\hat{\mathbf{n}}) Y_{l_2 m_2}(\hat{\mathbf{n}}) Y_{l_3 m_3}(\hat{\mathbf{n}}). \quad (7)$$

The physical role of the Gaunt integral is to assure that (l_1, m_1) , (l_2, m_2) , and (l_3, m_3) form a triangle. In the small-angle limit, the Gaunt integral becomes a 2-d delta function: $\mathcal{G}_{l_1 l_2 l_3}^{m_1 m_2 m_3} \rightarrow (2\pi)^2 \delta^D(\mathbf{l}_1 + \mathbf{l}_2 + \mathbf{l}_3)$ [77].

Given this parametrization, one can then maximize the PDF given in equation 5 with respect to $f_{\text{NL}}^{(i)}$ by solving $d \ln P / df_{\text{NL}}^{(i)} = 0$ and find the optimal estimator:

$$f_{\text{NL}}^{(i)} = \sum_j (F^{-1})_{ij} S_j. \quad (8)$$

One can use this formula to determine multiple amplitudes of angular bispectra simultaneously.

Here, S_i are given by the data as

$$S_i \equiv \frac{1}{6} \sum_{\text{all } lm} \mathcal{G}_{l_1 l_2 l_3}^{m_1 m_2 m_3} b_{l_1 l_2 l_3}^{(i)} \times \left[(C^{-1}a)_{l_1 m_1} (C^{-1}a)_{l_2 m_2} (C^{-1}a)_{l_3 m_3} - 3(C^{-1})_{l_1 m_1, l_2 m_2} (C^{-1}a)_{l_3 m_3} \right], \quad (9)$$

where $1/6$ is included such that F_{ij} in equation 8 becomes the Fisher matrix of $f_{\text{NL}}^{(i)}$. In other words, the covariance matrix of $f_{\text{NL}}^{(i)}$ is given by the inverse of F_{ij} , i.e.,

$$(F^{-1})_{ij} = \langle f_{\text{NL}}^{(i)} f_{\text{NL}}^{(j)} \rangle - \langle f_{\text{NL}}^{(i)} \rangle \langle f_{\text{NL}}^{(j)} \rangle. \quad (10)$$

The 68% uncertainty in $f_{\text{NL}}^{(i)}$ is given by $\Delta f_{\text{NL}}^{(i)} = (F^{-1})_{ii}$.

Using the definition of the Gaunt integral given in equation 7, we rewrite S_i as

$$S_i = \frac{1}{6} \int d^2 \hat{\mathbf{n}} \sum_{l_1 l_2 l_3} b_{l_1 l_2 l_3}^{(i)} [e_{l_1}(\hat{\mathbf{n}}) e_{l_2}(\hat{\mathbf{n}}) e_{l_3}(\hat{\mathbf{n}}) - 3d_{l_1 l_2}(\hat{\mathbf{n}}) e_{l_3}(\hat{\mathbf{n}})], \quad (11)$$

where

$$e_l(\hat{\mathbf{n}}) \equiv \sum_m (C^{-1}a)_{lm} Y_{lm}(\hat{\mathbf{n}}), \quad (12)$$

$$d_{ll'}(\hat{\mathbf{n}}) \equiv \sum_{mm'} (C^{-1})_{lm,l'm'} Y_{lm}(\hat{\mathbf{n}}) Y_{l'm'}(\hat{\mathbf{n}}). \quad (13)$$

Here, the summation over m can be done using the Fast Fourier Transform (FFT), as $Y_{lm}(\theta, \phi) \propto e^{im\phi}$. This technique is used by the **HEALPix** package [78], and thus one may use **HEALPix** to do this summation. To compute $d_{ll'}(\hat{\mathbf{n}})$, one may use Monte Carlo simulations. Namely, as $C_{lm,l'm'} = \langle a_{lm}^* a_{l'm'} \rangle$, we have the exact relation between $d_{ll'}$ and e_l : $d_{ll'}(\hat{\mathbf{n}}) = \langle e_l(\hat{\mathbf{n}}) e_{l'}(\hat{\mathbf{n}}) \rangle$. One can evaluate the ensemble average using the Monte Carlo simulation of the CMB and the instrumental noise. Let us denote this operation by $d_{ll'}(\hat{\mathbf{n}}) = \langle e_l(\hat{\mathbf{n}}) e_{l'}(\hat{\mathbf{n}}) \rangle_{\text{MC}}$. The final formula for S_i is

$$S_i = \frac{1}{6} \int d^2\hat{\mathbf{n}} \sum_{l_1 l_2 l_3} b_{l_1 l_2 l_3}^{(i)} [e_{l_1}(\hat{\mathbf{n}}) e_{l_2}(\hat{\mathbf{n}}) e_{l_3}(\hat{\mathbf{n}}) - 3e_{l_3}(\hat{\mathbf{n}}) \langle e_{l_1}(\hat{\mathbf{n}}) e_{l_2}(\hat{\mathbf{n}}) \rangle_{\text{MC}}] \quad (14)$$

which is valid for general forms of $b_{l_1 l_2 l_3}^{(i)}$. Note that the integral, $\int d^2\hat{\mathbf{n}}$, must be done over the full sky, even in the presence of the mask: the information on the mask is included in the calculation of the Fisher matrix, F_{ij} . The only assumptions that we have made so far are: (1) each angular bispectrum component has only one free parameter, i.e., the amplitude, and (2) non-Gaussianity (if any) is weak, and the PDF of a_{lm} is given by equation 5.

Finally, the explicit form of the Fisher matrix is given by

$$F_{ij} = \frac{f_{\text{sky}}}{6} \sum_{\text{all } l'm} \sum_{\text{all } l'm'} \mathcal{G}_{l_1 l_2 l_3}^{m_1 m_2 m_3} b_{l_1 l_2 l_3}^{(i)} \times (C^{-1})_{l_1 m_1, l'_1 m'_1} (C^{-1})_{l_2 m_2, l'_2 m'_2} (C^{-1})_{l_3 m_3, l'_3 m'_3} b_{l'_1 l'_2 l'_3}^{(j)} \mathcal{G}_{l'_1 l'_2 l'_3}^{m'_1 m'_2 m'_3}, \quad (15)$$

where f_{sky} is the fraction of the sky outside of the mask. When the covariance matrix is diagonal, the expression simplifies to

$$F_{ij} = \frac{f_{\text{sky}}}{6} \sum_{\text{all } l} I_{l_1 l_2 l_3} \frac{b_{l_1 l_2 l_3}^{(i)} b_{l_1 l_2 l_3}^{(j)}}{C_{l_1} C_{l_2} C_{l_3}}, \quad (16)$$

where

$$I_{l_1 l_2 l_3} \equiv \sum_{\text{all } m} (\mathcal{G}_{l_1 l_2 l_3}^{m_1 m_2 m_3})^2 = \frac{(2l_1 + 1)(2l_2 + 1)(2l_3 + 1)}{4\pi} \begin{pmatrix} l_1 & l_2 & l_3 \\ 0 & 0 & 0 \end{pmatrix}^2. \quad (17)$$

Equation 16 may also be written as

$$F_{ij} = f_{\text{sky}} \sum_{l_3 \leq l_2 \leq l_1} I_{l_1 l_2 l_3} \frac{b_{l_1 l_2 l_3}^{(i)} b_{l_1 l_2 l_3}^{(j)}}{C_{l_1} C_{l_2} C_{l_3} \Delta_{l_1 l_2 l_3}}, \quad (18)$$

where $\Delta_{l_1 l_2 l_3} = 1, 2$, and 6 when all of l_i 's are different, two of l'_i are the same, and all of l_i 's are the same, respectively.

3.2. Poisson bispectrum

As a warm up, let us consider the simplest example: point sources randomly distributed over the sky. As mentioned already, this is a contamination of the primordial non-Gaussianity parameters, and thus an accurate measurement of this component is quite important, especially for *Planck* as well as for the South Pole Telescope (SPT) and Atacama Cosmology Telescope (ACT), which are working at high frequencies ($\nu > 100$ GHz) where star-forming galaxies dominate a_{lm} at $l > 1000$.

For the Poisson distribution, the reduced bispectrum is independent of multipoles, $b_{l_1 l_2 l_3}^{\text{src}} = 1$, in the absence of window functions, and is given by

$$b_{l_1 l_2 l_3}^{\text{src}} = w_{l_1} w_{l_2} w_{l_3}, \quad (19)$$

in the presence window functions. Here, w_l is an experimental window function (a product of the beam transfer function and the pixel window function). Let us then use b_{src} (instead of f_{NL} because this component has nothing to do with primordial fluctuations) to denote the amplitude of the Poisson bispectrum.

From the data, we measure S_{src} given by

$$S_{\text{src}} = \frac{1}{6} \int d^2 \hat{\mathbf{n}} \left[E^3(\hat{\mathbf{n}}) - 3E(\hat{\mathbf{n}}) \langle E^2(\hat{\mathbf{n}}) \rangle_{\text{MC}} \right], \quad (20)$$

where a map $E(\hat{\mathbf{n}})$ is defined by [79]

$$E(\hat{\mathbf{n}}) \equiv \sum_l w_l e_l(\hat{\mathbf{n}}) = \sum_{lm} w_l (C^{-1}a)_{lm} Y_{lm}(\hat{\mathbf{n}}). \quad (21)$$

3.3. Primordial bispectra

(Most of this subsection is adopted from Section 6.1 of [11].) During the period of cosmic inflation [81–86], quantum fluctuations were generated and became the seeds for the cosmic structures that we observe today [82, 87–90]. See [91–96] for reviews.

Inflation predicts that the statistical distribution of primordial fluctuations is nearly a Gaussian distribution with random phases. Measuring deviations from a Gaussian distribution, i.e., non-Gaussian correlations in primordial fluctuations, is a powerful test of inflation, as how precisely the distribution is (non-)Gaussian depends on the detailed physics of inflation. See [2, 70] for reviews.

The observed angular bispectrum is related to the 3-dimensional bispectrum of primordial curvature perturbations, $\langle \zeta_{\mathbf{k}_1} \zeta_{\mathbf{k}_2} \zeta_{\mathbf{k}_3} \rangle = (2\pi)^3 \delta^D(\mathbf{k}_1 + \mathbf{k}_2 + \mathbf{k}_3) B_\zeta(k_1, k_2, k_3)$. In the linear order, the primordial curvature perturbation is related to Bardeen's curvature perturbation [97] in the matter-dominated era, Φ , by $\zeta = \frac{5}{3}\Phi$ [98]. The CMB temperature anisotropy in the Sachs–Wolfe limit [99] is given by $\Delta T/T = -\frac{1}{3}\Phi = -\frac{1}{5}\zeta$. We write the bispectrum of Φ as

$$\langle \Phi(\mathbf{k}_1) \Phi(\mathbf{k}_2) \Phi(\mathbf{k}_3) \rangle = (2\pi)^3 \delta^D(\mathbf{k}_1 + \mathbf{k}_2 + \mathbf{k}_3) F(k_1, k_2, k_3). \quad (22)$$

There is a useful way of visualizing the shape dependence of the bispectrum. We can study the structure of the bispectrum by plotting the magnitude of $F(k_1, k_2, k_3) (k_2/k_1)^2 (k_3/k_1)^2$ as a function of k_2/k_1 and k_3/k_1 for a given k_1 , with

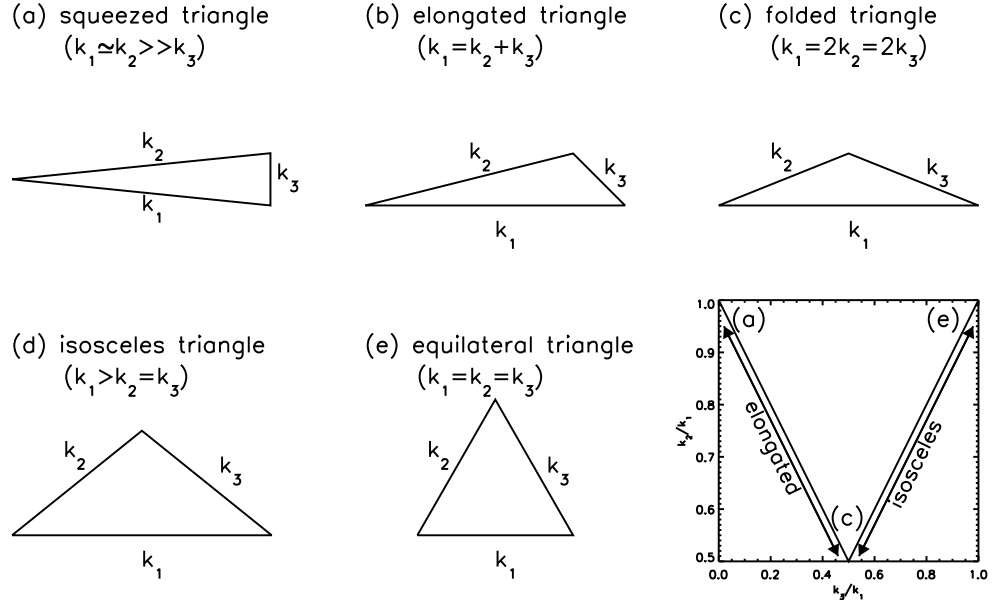


Figure 2. Visual representations of triangles forming the bispectrum, $B_\Phi(k_1, k_2, k_3)$, with various combinations of wavenumbers satisfying $k_3 \leq k_2 \leq k_1$. This figure is adopted from [80].

a condition that $k_1 \geq k_2 \geq k_3$ is satisfied. In order to classify various shapes of the triangles, let us use the following names: squeezed ($k_1 \simeq k_2 \gg k_3$), elongated ($k_1 = k_2 + k_3$), folded ($k_1 = 2k_2 = 2k_3$), isosceles ($k_2 = k_3$), and equilateral ($k_1 = k_2 = k_3$). See (a)–(e) of Figure 2 for the visual representations of these triangles.

We shall explore 3 different shapes of the primordial bispectrum: “local,” “equilateral,” and “orthogonal.” They are defined as follows:

1. **Local form.** The local form bispectrum is given by [76, 100, 101]

$$\begin{aligned}
 & F_{\text{local}}(k_1, k_2, k_3) \\
 &= 2f_{\text{NL}}^{\text{local}}[P_\Phi(k_1)P_\Phi(k_2) + P_\Phi(k_2)P_\Phi(k_3) + P_\Phi(k_3)P_\Phi(k_1)] \\
 &= 2A^2 f_{\text{NL}}^{\text{local}} \left[\frac{1}{k_1^{4-n_s} k_2^{4-n_s}} + (\text{2 perm.}) \right], \tag{23}
 \end{aligned}$$

where $P_\Phi = A/k^{4-n_s}$ is the power spectrum of Φ with a normalization factor A . This form is called the local form, as this bispectrum can arise from the curvature perturbation in the form of $\Phi = \Phi_L + f_{\text{NL}}^{\text{local}}\Phi_L^2$, where both sides are evaluated at the same location in space (Φ_L is a linear Gaussian fluctuation).[§] The local

[§] However, $\Phi = \Phi_L + f_{\text{NL}}^{\text{local}}\Phi_L^2$ is not the only way to produce this type of bispectrum. One can also produce this form from multi-scalar field inflation models where scalar field fluctuations are nearly scale invariant [22]; multi-scalar models called “curvaton” scenarios [20, 102]; multi-field models in which one field modulates the decay rate of inflaton field [21, 103, 104]; multi-field models in which a violent production of particles and non-linear reheating, called “preheating,” occur due to parametric resonances [24, 105–107]; models in which the universe contracts first and then bounces [23].

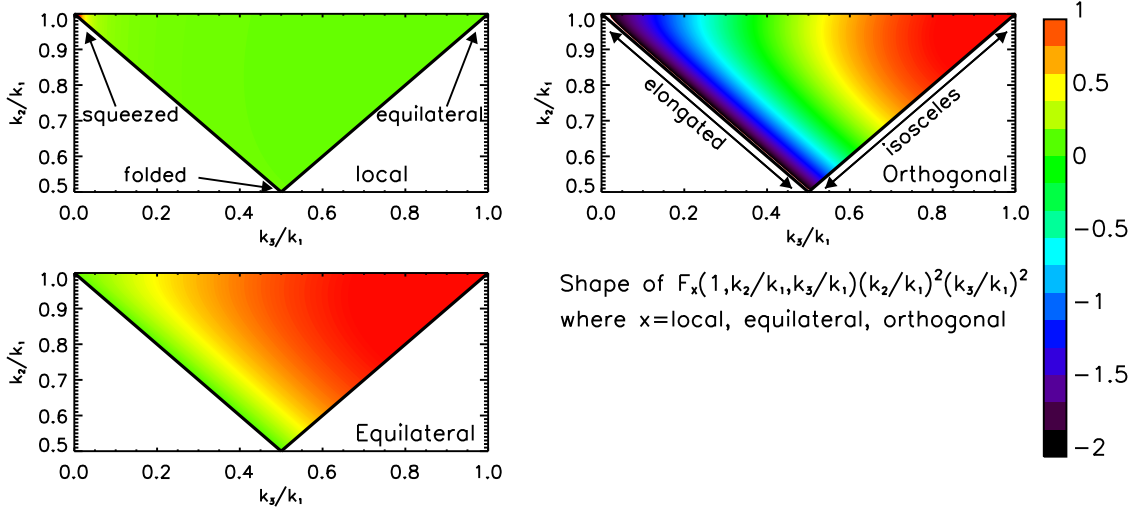


Figure 3. Shapes of the primordial bispectra. Each panel shows the normalized amplitude of $F(k_1, k_2, k_3)(k_2/k_1)^2(k_3/k_1)^2$ as a function of k_2/k_1 and k_3/k_1 for a given k_1 , with a condition that $k_3 \leq k_2 \leq k_1$ is satisfied. As the primordial bispectra shown here are (nearly) scale invariant, the shapes look similar regardless of the values of k_1 . The amplitude is normalized such that it is unity at the point where $F(k_1, k_2, k_3)(k_2/k_1)^2(k_3/k_1)^2$ takes on the maximum value. (Top Left) The local form given in equation 23, which peaks at the squeezed configuration. Note that the most squeezed configuration shown here has $k_1 = k_2 = 100k_3$. (Top Right) The orthogonal form given in equation 27, which has a positive peak at the equilateral configuration, and a negative valley along the elongated configurations. (Bottom Left) The equilateral form given in equation 26, which peaks at the equilateral configuration. Note that all of these shapes are nearly orthogonal to each other.

form, $F_{\text{local}}(k_1, k_2, k_3)(k_2/k_1)^2(k_3/k_1)^2$, peaks at the so-called ‘‘squeezed’’ triangle for which $k_3 \ll k_2 \approx k_1$ [18]. See the top-left panel of Figure 3. In this limit, we obtain

$$F_{\text{local}}(k_1, k_1, k_3 \rightarrow 0) = 4f_{\text{NL}}^{\text{local}} P_{\Phi}(k_1) P_{\Phi}(k_3). \quad (24)$$

How large is $f_{\text{NL}}^{\text{local}}$ from inflation? The earlier calculations showed that $f_{\text{NL}}^{\text{local}}$ from single-field slow-roll inflation would be of order the slow-roll parameter, $\epsilon \sim 10^{-2}$ [100, 108, 109]. More recently, Maldacena [3] and Acquaviva et al. [4] found that the coefficient of $P_{\Phi}(k_1) P_{\Phi}(k_3)$ from the simplest single-field slow-roll inflation with the canonical kinetic term in the squeezed limit is given by

$$F_{\text{local}}(k_1, k_1, k_3 \rightarrow 0) = \frac{5}{3}(1 - n_s) P_{\Phi}(k_1) P_{\Phi}(k_3). \quad (25)$$

Comparing this result with the form predicted by the $f_{\text{NL}}^{\text{local}}$ model, one obtains $f_{\text{NL}}^{\text{local}} = (5/12)(1 - n_s)$, which gives $f_{\text{NL}}^{\text{local}} = 0.015$ for $n_s = 0.963$.

2. Equilateral form. The equilateral form bispectrum is given by [7]

$$F_{\text{equil}}(k_1, k_2, k_3)$$

$$= 6A^2 f_{\text{NL}}^{\text{equil}} \left\{ -\frac{1}{k_1^{4-n_s} k_2^{4-n_s}} - \frac{1}{k_2^{4-n_s} k_3^{4-n_s}} - \frac{1}{k_3^{4-n_s} k_1^{4-n_s}} \right. \\ \left. - \frac{2}{(k_1 k_2 k_3)^{2(4-n_s)/3}} + \left[\frac{1}{k_1^{(4-n_s)/3} k_2^{2(4-n_s)/3} k_3^{4-n_s}} + (\text{5 perm.}) \right] \right\} \quad (26)$$

This function approximates the bispectrum forms that arise from a class of inflation models in which scalar fields have non-canonical kinetic terms. One example is the so-called Dirac-Born-Infeld (DBI) inflation [26, 110], which gives $f_{\text{NL}}^{\text{equil}} \propto -1/c_s^2$ in the limit of $c_s \ll 1$, where c_s is the effective sound speed at which scalar field fluctuations propagate. There are various other models that can produce $f_{\text{NL}}^{\text{equil}}$ [19, 27, 28, 111, 112]. The equilateral form, $F_{\text{equil}}(k_1, k_2, k_3)(k_2/k_1)^2(k_3/k_1)^2$, peaks at the equilateral configuration for which $k_1 = k_2 = k_3$. See the bottom-left panel of Figure 3. The local and equilateral forms are nearly orthogonal to each other, which means that both can be measured nearly independently.

3. **Orthogonal form.** The orthogonal form, which is constructed such that it is nearly orthogonal to both the local and equilateral forms, is given by [31]

$$F_{\text{orthog}}(k_1, k_2, k_3) \\ = 6A^2 f_{\text{NL}}^{\text{orthog}} \left\{ -\frac{3}{k_1^{4-n_s} k_2^{4-n_s}} - \frac{3}{k_2^{4-n_s} k_3^{4-n_s}} - \frac{3}{k_3^{4-n_s} k_1^{4-n_s}} \right. \\ \left. - \frac{8}{(k_1 k_2 k_3)^{2(4-n_s)/3}} + \left[\frac{3}{k_1^{(4-n_s)/3} k_2^{2(4-n_s)/3} k_3^{4-n_s}} + (\text{5 perm.}) \right] \right\} \quad (27)$$

This form approximates the forms that arise from a linear combination of higher-derivative scalar-field interaction terms, each of which yields forms similar to the equilateral shape. Senatore, Smith and Zaldarriaga [31] found that, using the “effective field theory of inflation” approach [111], a certain linear combination of similarly equilateral shapes can yield a distinct shape which is orthogonal to both the local and equilateral forms. The orthogonal form, $F_{\text{orthog}}(k_1, k_2, k_3)(k_2/k_1)^2(k_3/k_1)^2$, has a positive peak at the equilateral configuration, and a negative valley along the elongated configurations. See the top-right panel of Figure 3.

Note that these are not the most general forms one can write down, and there are other forms which would probe different aspects of the physics of inflation [19, 29, 32, 36, 63, 113].

Of these forms, the local form bispectrum has special significance. Creminelli and Zaldarriaga [5] showed that not only models with the canonical kinetic term, but *all* single-inflation models predict the bispectrum in the squeezed limit given by equation 25, regardless of the form of potential, kinetic term, slow-roll, or initial vacuum state. Also see [19, 28, 111]. This means that a convincing detection of $f_{\text{NL}}^{\text{local}}$ would rule out *all* single-field inflation models.

3.4. Optimal estimator for $f_{\text{NL}}^{\text{local}}$

Given the form of Φ , one can calculate the harmonic coefficients of temperature and E -mode polarization anisotropies as

$$a_{lm}^T = 4\pi(-i)^l \int \frac{d^3\mathbf{k}}{(2\pi)^3} \Phi(\mathbf{k}) g_{Tl}(k) Y_{lm}^*(\mathbf{k}), \quad (28)$$

$$a_{lm}^E = 4\pi(-i)^l \sqrt{\frac{(l+2)!}{(l-2)!}} \int \frac{d^3\mathbf{k}}{(2\pi)^3} \Phi(\mathbf{k}) g_{Pl}(k) Y_{lm}^*(\mathbf{k}), \quad (29)$$

where $g_{Tl}(k)$ and $g_{Pl}(k)$ are the radiation transfer functions of the temperature and polarization anisotropies, respectively, which can be calculated by solving the linearized Boltzmann equations. One may use the publicly-available Boltzmann codes such as **CMBFAST** [114] or **CAMB** [115] for computing the radiation transfer functions.||

From now on, we shall focus on the temperature anisotropy, largely for simplicity. (See [116, 117] for the treatment of polarization in the angular bispectrum.) The limits on f_{NL} expected from *Planck* are dominated by the temperature information, and thus the polarization information is not expected to yield competitive limits over the next, say, > 5 years.

For the local-form bispectrum given in equation 23, the reduced bispectrum (equation 6) is given by [76]

$$b_{l_1 l_2 l_3}^{\text{local}} = 2 \int r^2 dr [\beta_{l_1}(r) \beta_{l_2}(r) \alpha_{l_3}(r) + (\text{2 perm.})] w_{l_1} w_{l_2} w_{l_3}, \quad (30)$$

where

$$\alpha_l(r) = \frac{2}{\pi} \int k^2 dk g_{Tl}(k) j_l(kr), \quad (31)$$

$$\beta_l(r) = \frac{2}{\pi} \int k^2 dk P_\Phi(k) g_{Tl}(k) j_l(kr). \quad (32)$$

Using this form in equation 14, one finds S_{local} as

$$S_{\text{local}} = \int r^2 dr \int d^2\hat{\mathbf{n}} \left[A(\hat{\mathbf{n}}, r) B^2(\hat{\mathbf{n}}, r) - 2B(\hat{\mathbf{n}}) \langle A(\hat{\mathbf{n}}, r) B(\hat{\mathbf{n}}, r) \rangle_{\text{MC}} \right. \\ \left. - A(\hat{\mathbf{n}}, r) \langle B^2(\hat{\mathbf{n}}, r) \rangle_{\text{MC}} \right], \quad (33)$$

which can be measured from the data. Here, maps $A(\hat{\mathbf{n}})$ and $B(\hat{\mathbf{n}})$ are defined by [6]

$$A(\hat{\mathbf{n}}) \equiv \sum_l w_l \alpha_l(r) e_l(\hat{\mathbf{n}}) = \sum_{lm} w_l \alpha_l(r) (C^{-1}a)_{lm} Y_{lm}(\hat{\mathbf{n}}), \quad (34)$$

$$B(\hat{\mathbf{n}}) \equiv \sum_l w_l \beta_l(r) e_l(\hat{\mathbf{n}}) = \sum_{lm} w_l \beta_l(r) (C^{-1}a)_{lm} Y_{lm}(\hat{\mathbf{n}}). \quad (35)$$

|| A CMBFAST-based code for computing $g_{Tl}(k)$ and $g_{Pl}(k)$ is available at <http://gyudon.as.utexas.edu/~komatsu/CRL>. A recent version of **CAMB** has an option to calculate these functions (<http://camb.info>).

3.5. Optimal estimator for $f_{\text{NL}}^{\text{equil}}$

For the equilateral-form bispectrum given in equation 26, the reduced bispectrum is given by [7]

$$b_{l_1 l_2 l_3}^{\text{equil}} = -3b_{l_1 l_2 l_3}^{\text{local}} + 6 \int r^2 dr [\beta_{l_1}(r) \gamma_{l_2}(r) \delta_{l_3}(r) + (\text{5 perm.}) \\ - 2\delta_{l_1}(r) \delta_{l_2}(r) \delta_{l_3}(r)] w_{l_1} w_{l_2} w_{l_3}, \quad (36)$$

where

$$\gamma_l(r) = \frac{2}{\pi} \int k^2 dk P_{\Phi}^{1/3}(k) g_{Tl}(k) j_l(kr), \quad (37)$$

$$\delta_l(r) = \frac{2}{\pi} \int k^2 dk P_{\Phi}^{2/3}(k) g_{Tl}(k) j_l(kr). \quad (38)$$

Using this form in equation 14, one finds S_{equil} as

$$S_{\text{equil}} = -3S_{\text{local}} + 6 \int r^2 dr \int d^2 \hat{\mathbf{n}} \{ B(\hat{\mathbf{n}}, r) C(\hat{\mathbf{n}}, r) D(\hat{\mathbf{n}}, r) \\ - B(\hat{\mathbf{n}}) \langle C(\hat{\mathbf{n}}, r) D(\hat{\mathbf{n}}, r) \rangle_{\text{MC}} - C(\hat{\mathbf{n}}) \langle B(\hat{\mathbf{n}}, r) D(\hat{\mathbf{n}}, r) \rangle_{\text{MC}} \\ - D(\hat{\mathbf{n}}) \langle B(\hat{\mathbf{n}}, r) C(\hat{\mathbf{n}}, r) \rangle_{\text{MC}} - \frac{1}{3} [D^3(\hat{\mathbf{n}}, r) - 3D(\hat{\mathbf{n}}) \langle D^2(\hat{\mathbf{n}}, r) \rangle_{\text{MC}}] \}, \quad (39)$$

which can be measured from the data. Here, maps $C(\hat{\mathbf{n}})$ and $D(\hat{\mathbf{n}})$ are defined by [7]

$$C(\hat{\mathbf{n}}) \equiv \sum_l w_l \gamma_l(r) e_l(\hat{\mathbf{n}}) = \sum_{lm} w_l \gamma_l(r) (C^{-1} a)_{lm} Y_{lm}(\hat{\mathbf{n}}), \quad (40)$$

$$D(\hat{\mathbf{n}}) \equiv \sum_l w_l \delta_l(r) e_l(\hat{\mathbf{n}}) = \sum_{lm} w_l \delta_l(r) (C^{-1} a)_{lm} Y_{lm}(\hat{\mathbf{n}}). \quad (41)$$

3.6. Optimal estimator for $f_{\text{NL}}^{\text{orthog}}$

For the equilateral-form bispectrum given in equation 27, the reduced bispectrum is given by [31]

$$b_{l_1 l_2 l_3}^{\text{orthog}} = 3b_{l_1 l_2 l_3}^{\text{equil}} - 12 \int r^2 dr \delta_{l_1}(r) \delta_{l_2}(r) \delta_{l_3}(r) w_{l_1} w_{l_2} w_{l_3}. \quad (42)$$

Using this form in equation 14, one finds S_{orthog} as

$$S_{\text{orthog}} = 3S_{\text{equil}} - 2 \int r^2 dr \int d^2 \hat{\mathbf{n}} [D^3(\hat{\mathbf{n}}, r) - 3D(\hat{\mathbf{n}}) \langle D^2(\hat{\mathbf{n}}, r) \rangle_{\text{MC}}], \quad (43)$$

which can be measured from the data.

4. Secondary anisotropy

4.1. General formula for the lensing-secondary coupling

Given the special importance of the local-form bispectrum, we must understand what other (non-primordial) effects might also produce the local form, potentially preventing us from measuring $f_{\text{NL}}^{\text{local}}$.

The local-form bispectrum is generated when the power spectrum of short-wavelength fluctuations is modulated by long-wavelength fluctuations; thus, a

mechanism that couples small scales to large scales can potentially generate the local-form bispectrum.

The weak gravitational lensing provides one such mechanism. The local-form bispectrum may then be generated when long- and short-wavelength fluctuations are coupled by the lensing. To see how this might happen, let us write the observed temperature anisotropy in terms of the original (unlensed) contribution from the last scattering surface at $z = 1090$, ΔT^P (where “ P ” stands for “*primary*”), the lensing potential, ϕ , and the secondary anisotropy generated between $z = 1090$ and $z = 0$, ΔT^S (where “ S ” stands for “*secondary*”):

$$\begin{aligned}\Delta T(\hat{\mathbf{n}}) &= \Delta T^P(\hat{\mathbf{n}} + \vec{\partial}\phi) + \Delta T^S(\hat{\mathbf{n}}) \\ &\approx \Delta T^P(\hat{\mathbf{n}}) + [(\vec{\partial}\phi) \cdot (\vec{\partial}\Delta T^P)](\hat{\mathbf{n}}) + \Delta T^S(\hat{\mathbf{n}}),\end{aligned}\quad (44)$$

where

$$\phi(\hat{\mathbf{n}}) = -2 \int_0^{r_*} dr \frac{r_* - r}{rr_*} \Phi(r, \hat{\mathbf{n}}r), \quad (45)$$

and r_* is the comoving distance out to $z = 1090$, and Φ is Bardeen’s curvature perturbation, which is related to the usual Newtonian gravitational potential by $\Phi = -\Phi_{\text{Newton}}$. Transforming this into harmonic space and computing the reduced bispectrum, one obtains [12]

$$b_{l_1 l_2 l_3}^{\text{lens-S}} = \left[\frac{l_1(l_1 + 1) - l_2(l_2 + 1) + l_3(l_3 + 1)}{2} C_{l_1}^P C_{l_3}^{\phi S} + (\text{5 perm.}) \right] w_{l_1} w_{l_2} w_{l_3}, \quad (46)$$

where C_l^P is the power spectrum of the CMB *from the decoupling epoch only* (i.e., no ISW), and $C_l^{\phi S} \equiv \langle \phi_{lm}^* a_{lm}^S \rangle$ is the lensing-secondary cross-correlation power spectrum.

From this result, one finds that a non-zero bispectrum is generated when the secondary anisotropy traces the large-scale structure (i.e., Φ). Various secondary effects have been studied in the literature: the Sunyaev–Zel’dovich effect [12], cosmic reionization [118], point sources [119], and ISW [12]. It has been shown that the last one, the ISW-lensing coupling, is the most dominant contamination of $f_{\text{NL}}^{\text{local}}$ [14].

Using equation 46 in equation 14, one finds $S_{\text{lens-S}}$ as

$$\begin{aligned}S_{\text{lens-S}} &= \frac{1}{2} \int d^2 \hat{\mathbf{n}} \left\{ P(\hat{\mathbf{n}}) [\partial^2 E](\hat{\mathbf{n}}) Q(\hat{\mathbf{n}}) \right. \\ &\quad \left. - [\partial^2 P](\hat{\mathbf{n}}) E(\hat{\mathbf{n}}) Q(\hat{\mathbf{n}}) - P(\hat{\mathbf{n}}) E(\hat{\mathbf{n}}) [\partial^2 Q](\hat{\mathbf{n}}) \right. \\ &\quad \left. + (\text{linear terms}) \right\},\end{aligned}\quad (47)$$

$$(48)$$

which can be measured from the data. Here, the “linear terms” contain 9 terms with $\langle \rangle_{\text{MC}}$, such as $-P(\hat{\mathbf{n}}) \langle [\partial^2 E](\hat{\mathbf{n}}) Q(\hat{\mathbf{n}}) \rangle_{\text{MC}}$, etc. The map $E(\hat{\mathbf{n}})$ is given by equation 21, and the other maps are defined by

$$P(\hat{\mathbf{n}}) \equiv \sum_l w_l C_l^P e_l(\hat{\mathbf{n}}) = \sum_{lm} w_l C_l^P (C^{-1} a)_{lm} Y_{lm}(\hat{\mathbf{n}}), \quad (49)$$

$$Q(\hat{\mathbf{n}}) \equiv \sum_l w_l C_l^{\phi S} e_l(\hat{\mathbf{n}}) = \sum_{lm} w_l C_l^{\phi S} (C^{-1} a)_{lm} Y_{lm}(\hat{\mathbf{n}}). \quad (50)$$

The maps with ∂^2 are given by $\partial^2 P = -\sum_l l(l+1) w_l C_l^P e_l(\hat{\mathbf{n}})$, etc. The map $P(\hat{\mathbf{n}})$ is a Wiener-filtered map of the primary temperature anisotropy from $z = 1090$.

4.2. Lensing-ISW coupling

A change in the curvature perturbation yields a secondary temperature anisotropy via the ISW effect [99]:

$$\frac{\Delta T^{\text{ISW}}(\hat{\mathbf{n}})}{T} = -2 \int_0^{r_*} dr \frac{\partial \Phi}{\partial r}(r, \hat{\mathbf{n}}r), \quad (51)$$

where r is the comoving distance and r_* is the comoving distance out to $z = 1090$. Here, note again $\Phi = -\Phi_{\text{Newton}}$. The cross-power spectrum of ϕ and the ISW effect is then given by

$$C_l^{\phi, \text{ISW}} = 4 \int_0^{r_*} dr \frac{r_* - r}{r_* r^3} P_{\Phi \Phi'} \left(\frac{l}{r}, r \right), \quad (52)$$

where $P_{\Phi \Phi'}(k, r)$ is the cross-power spectrum of Φ and $\Phi' \equiv \partial \Phi / \partial r$, which can be calculated from the power spectrum of Φ , $P_\Phi(k, r)$, as $P_{\Phi \Phi'}(k, r) = \frac{1}{2} [\partial P_\Phi(k, r) / \partial r]$ [13, 120]. Here, $P_\Phi(k, r)$ is not the primordial power spectrum, but it includes the linear transfer function, $T(k)$, and the growth factor of Φ , $g(r)$:

$$P_\Phi(k, r) = \frac{A}{k^{4-n_s}} [T(k)g(r)]^2. \quad (53)$$

Using this, one finds $P_{\Phi \Phi'}(k, r) = (g'/g)P_\Phi(k, r)$. Note that $g(r)$ is normalized such that $g(r) = 1$ during the matter-dominated era.

With this result, it is easy to see why the lensing-ISW coupling yields the squeezed configuration: on very large scales, where $T(k) \rightarrow 1$, $C_l^{\phi, \text{ISW}} \propto 1/l^3$. On smaller scales, $T(k)$ declines with k , and thus $C_l^{\phi, \text{ISW}}$ falls faster than $1/l^3$. The lensing coupling includes $l(l+1)C_l^{\phi, \text{ISW}}$, which falls faster than $1/l$, i.e., the largest power comes from the smallest l .

A recent estimate by Hanson et al. [15] showed that the lensing-ISW coupling, *if not included in the parameter estimation*, would bias $f_{\text{NL}}^{\text{local}}$ by $\Delta f_{\text{NL}}^{\text{local}} = 9.3$. The expected bias for WMAP is $\Delta f_{\text{NL}}^{\text{local}} = 2.7$ [11]. One can remove this bias by including the lensing-ISW coupling (or any other lensing-secondary couplings) using the optimal estimator given by equation 48.

5. Second-order effect

5.1. General discussion

So far, we have assumed that one can use equation 28:

$$a_{lm} = 4\pi(-i)^l \int \frac{d^3 \mathbf{k}}{(2\pi)^3} \Phi_p(\mathbf{k}) g_{Tl}(k) Y_{lm}^*(\mathbf{k}),$$

to convert the primordial curvature perturbation to the temperature anisotropy. (Here, the subscript “p” stands for “*primordial*,” by which we mean $\Phi_p = \frac{3}{5}\zeta$ without the linear transfer function.) However, this equation is valid only for linear theory. As *any* non-linear effects can produce non-Gaussianity, one has to study the impacts of various non-linear effects on the observed non-Gaussianity.

The origin of the linear radiation transfer function is the linearized Boltzmann equation:

$$\frac{\partial \Delta^{(1)}}{\partial \eta} + ik\mu\Delta^{(1)} + \sigma_T n_e a \Delta^{(1)} = S^{(1)}(k, \mu, \eta), \quad (54)$$

where η is the conformal time, $\mu \equiv \hat{\mathbf{k}} \cdot \hat{\mathbf{n}}$, $\Delta^{(1)} \equiv 4[\Delta T^{(1)}(k, \mu, \eta)/T]$ is the perturbation in the photon energy density, and $S^{(1)}$ is the *linear source function*, which depends on the metric perturbations as well as on the density, velocity, pressure, and stress perturbations of matter and radiation in the universe and the photon polarization.

The second-order Boltzmann equation is then similarly written as

$$\frac{\partial \Delta^{(2)}}{\partial \eta} + ik\mu\Delta^{(2)} + \sigma_T n_e a \Delta^{(2)} = S^{(2)}(\mathbf{k}, \hat{\mathbf{n}}, \eta), \quad (55)$$

where $\Delta^{(2)} \equiv 8[\Delta T^{(2)}(\mathbf{k}, \hat{\mathbf{n}}, \eta)/T] + 12[\Delta T^{(1)}(k, \mu, \eta)/T]^2$, and $S^{(2)}$ is the *second-order source function*. Note that the azimuthal symmetry is lost at the second order, and thus the perturbations depend on the directions of \mathbf{k} and $\hat{\mathbf{n}}$ independently. In this case, the second-order a_{lm} is given by [121]

$$a_{lm}^{(2)} = \frac{4\pi}{8}(-i)^l \int \frac{d^3\mathbf{k}}{(2\pi)^3} \int \frac{d^3\mathbf{k}'}{(2\pi)^3} \int d^3\mathbf{k}'' \delta^D(\mathbf{k}' + \mathbf{k}'' - \mathbf{k}) \Phi_p^{(1)}(\mathbf{k}') \Phi_p^{(1)}(\mathbf{k}'') \\ \times \sum_{l'm'} F_{lm}^{l'm'}(\mathbf{k}', \mathbf{k}'', \mathbf{k}) Y_{l'm'}^*(\hat{\mathbf{k}}), \quad (56)$$

where $F_{lm}^{l'm'}$ is the second-order radiation transfer function, whose form is determined by the second-order source function, $S^{(2)}$, in the Boltzmann equation.

The shape of the second-order bispectrum, $\langle a_{l_1 m_2}^{(1)} a_{l_2 m_3}^{(1)} a_{l_3 m_3}^{(2)} \rangle$, is determined by the shape of the second-order radiation transfer function. If the second-order radiation transfer function vanishes in the squeezed limit, i.e., $F_{lm}^{l'm'}(\mathbf{k}', \mathbf{k}'', \mathbf{k}) \rightarrow 0$ for $\mathbf{k} \rightarrow 0$, then the CMB bispectrum would not peak at the squeezed configuration, and thus the resulting f_{NL}^{local} would be small.

The second-order source function is quite complicated [122–132], but it can be divided into two parts¶:

- (1) The terms given by the products of the first-order perturbations, such as $[\Phi^{(1)}]^2$.
- (2) The terms given by the “intrinsically second-order terms,” such as $\Phi^{(2)}$.

The intrinsically second-order terms are sourced by products of the first-order perturbations, and thus it is created by the late-time evolution of cosmological perturbations, whereas the terms in (1) are set by the initial conditions.

The contamination of f_{NL}^{local} due to the terms in (1) is small, $|f_{NL}^{\text{local}}| < 1$ [121]. Recently, Pitrou, Bernardeau and Uzan [131] reported a surprising result that the terms in (2) would give $f_{NL}^{\text{local}} \sim 5$ for the *Planck* data ($l_{\text{max}} = 2000$).

¶ This decomposition is not gauge invariant, and thus which terms belong to (1) or (2) depends on the gauge that one chooses. Therefore, one must specify the gauge when making such a decomposition. Our discussion in this section is based on the gauge choice made by Bartolo, Matarrese and Riotto [122, 123] and Pitrou, Uzan and Bernardeau [130, 131], which reduces to the Newtonian gauge at the linear order. This seems a convenient gauge, as the products of the first-order terms only give $|f_{NL}^{\text{local}}| < 1$ [121].

Why surprising? As the intrinsically second-order terms arise as a consequence of the late-time evolution of the cosmological perturbations, they are generated by the causal mechanism, i.e., gravity and hydrodynamics. It is difficult for the causal mechanism to generate the bispectrum in the squeezed configuration, as it requires very long wavelength perturbations to be coupled to short wavelength ones.

5.2. Newtonian calculation

As an example, let us consider the well-known second-order solution for $\Phi^{(2)}$ in the *sub-horizon limit*, i.e., $k \gg aH$, which is equivalent to taking the non-relativistic (Newtonian) limit. Here, the second-order Bardeen curvature perturbation is defined by $\Phi = \Phi^{(1)} + \frac{1}{2}\Phi^{(2)}$. The explicit solution is [130]⁺

$$\begin{aligned} \frac{1}{2}\Phi^{(2)}(\mathbf{k}, \eta) &= \frac{1}{6} \int \frac{d^3\mathbf{k}'}{(2\pi)^3} d^3\mathbf{k}'' \delta^D(\mathbf{k}' + \mathbf{k}'' - \mathbf{k}) \left(\frac{k'k''\eta}{k} \right)^2 \\ &\quad \times F_2^{(s)}(\mathbf{k}', \mathbf{k}'') \Phi^{(1)}(\mathbf{k}') \Phi^{(1)}(\mathbf{k}''), \end{aligned} \quad (57)$$

where the linear perturbation, $\Phi^{(1)}$, on the right hand side is constant during the matter dominated era, and the symmetrized function, $F_2^{(s)}$, is defined as

$$F_2^{(s)}(\mathbf{k}_1, \mathbf{k}_2) = \frac{5}{7} + \frac{\mathbf{k}_1 \cdot \mathbf{k}_2}{2k_1 k_2} \left(\frac{k_1}{k_2} + \frac{k_2}{k_1} \right) + \frac{2}{7} \left(\frac{\mathbf{k}_1 \cdot \mathbf{k}_2}{k_1 k_2} \right)^2. \quad (58)$$

This function vanishes in the squeezed limit, $\mathbf{k}_1 = -\mathbf{k}_2$, and thus the CMB bispectrum generated from $\Phi^{(2)}$ in the *Newtonian limit* is not given by the local form.

To see this, let us calculate

$$\langle \Phi(\mathbf{k}_1, \eta) \Phi(\mathbf{k}_2, \eta) \Phi(\mathbf{k}_3, \eta) \rangle = (2\pi)^3 \delta^D(\mathbf{k}_1 + \mathbf{k}_2 + \mathbf{k}_3) F_{2\text{nd}}(k_1, k_2, k_3, \eta), \quad (59)$$

where

$$F_{2\text{nd}}(k_1, k_2, k_3, \eta) = \frac{\eta^2}{3} \left[\left(\frac{k_1 k_2}{k_3} \right)^2 F_2^{(s)}(\mathbf{k}_1, \mathbf{k}_2) P_\Phi(k_1) P_\Phi(k_2) + (\text{2 perm.}) \right], \quad (60)$$

and $P_\Phi(k) = AT^2(k)/k^{4-n_s}$. The shape dependence of $F_{2\text{nd}}(k_1, k_2, k_3)(k_2/k_1)^2(k_3/k_1)^2$ is shown in Figure 4 for various values of k_1 (because $F_{2\text{nd}}$ is not scale invariant). The CMB data are sensitive to $k_1 < k_{\text{max}} \sim 0.2 h \text{ Mpc}^{-1} (l_{\text{max}}/2000)$. We find that the bispectrum peaks at the equilateral configuration on large scales ($k_1 < 10^{-2} h \text{ Mpc}^{-1}$), and it peaks along the elongated configurations on small scales ($k_1 \sim 0.1 h \text{ Mpc}^{-1}$). It peaks at the squeezed configuration on a very small scale ($k_1 \sim 1 h \text{ Mpc}^{-1}$), but these scales are not accessible by the CMB due to the Silk damping. Note that the most squeezed configuration shown in this Figure has $k_1 = k_2 = 100k_3$. The dominant shape changes with scales, as the linear transfer function, $T(k)$, declines with k , with the small-scale limit given by $T(k) \propto \ln k/k^2$. From these results, we expect the second-order effect in the Newtonian limit to yield only a small contamination of $f_{\text{NL}}^{\text{local}}$.

⁺ Note that our Φ is (-1) times Φ used in equation 72 of [130].

The dominant contribution to the second-order temperature anisotropy in the sub-horizon limit is given by the second-order Sachs-Wolfe effect [130]:*

$$\frac{\Delta T^{(2)}}{T}(\hat{\mathbf{n}}) = \frac{1}{2} R_* \Phi^{(2)}(r_*, \hat{\mathbf{n}} r_*), \quad (61)$$

where $R_* \equiv 3\rho_b/(4\rho_\gamma)$ is the baryon-photon ratio at the decoupling epoch. (Here, a factor of 1/2 comes from our way of defining the second-order temperature anisotropy, $\Delta T = \Delta T^{(1)} + \Delta T^{(2)}$ and the second-order curvature perturbation, $\Phi = \Phi^{(1)} + \frac{1}{2}\Phi^{(2)}$. This definition follows from Ref. [121].) The corresponding second-order a_{lm} is

$$\begin{aligned} a_{lm}^{(2)} &= 4\pi(-i)^l \int \frac{d^3\mathbf{k}}{(2\pi)^3} \left[\frac{1}{2} R_* \Phi^{(2)}(\mathbf{k}, \eta_*) \right] j_l(kr_*) Y_{lm}^*(\hat{\mathbf{k}}) \\ &= \frac{4\pi}{8} (-i)^l \int \frac{d^3\mathbf{k}}{(2\pi)^3} \int \frac{d^3\mathbf{k}'}{(2\pi)^3} d^3\mathbf{k}'' \delta^D(\mathbf{k}' + \mathbf{k}'' - \mathbf{k}) \Phi_p^{(1)}(\mathbf{k}') \Phi_p^{(1)}(\mathbf{k}'') \\ &\quad \times \sum_{l'm'} \left[\frac{4}{3} R_* \left(\frac{k'k''\eta_*}{k} \right)^2 F_2^{(s)}(\mathbf{k}', \mathbf{k}'') T(k') T(k'') j_l(kr_*) \delta_{ll'} \delta_{mm'} \right] Y_{l'm'}^*(\hat{\mathbf{k}}), \end{aligned} \quad (62)$$

where the linear primordial perturbation, $\Phi_p^{(1)}$, is related to $\Phi^{(1)}$ as $\Phi^{(1)}(\mathbf{k}) = \Phi_p^{(1)}(\mathbf{k})T(k)$. Comparing this with equation 56, we identify the term inside the square bracket as the second-order radiation transfer function, $F_{lm}^{l'm'}$.‡

With this result, one can calculate the reduced bispectrum of the Newtonian second-order effect, $b_{l_1 l_2 l_3}^{2\text{nd}}$. The resulting $f_{\text{NL}}^{\text{local}}$ is always less than unity regardless of the angular scales (D. Nitta 2010, private communication; also see [134]). The calculation was done for $l \leq 2000$.

How can we reconcile this result with those found in [131]? The difference between these results seems to imply that the most dominant contamination of $f_{\text{NL}}^{\text{local}}$ comes from the general relativistic (post Newtonian) evolution of $\Phi^{(2)}$ that is not captured by the above Newtonian calculation. This is yet to be confirmed; however, if this is true, one should be able to construct a simple template for the second-order bispectrum, and use it to remove the contamination by including its amplitude, $f_{\text{NL}}^{2\text{nd}}$, in the fit.

6. Four-point function: local-form trispectrum test of multi-field models

Widely used notation for the “local-form trispectrum” is

$$\begin{aligned} &\langle \Phi(\mathbf{k}_1) \Phi(\mathbf{k}_2) \Phi(\mathbf{k}_3) \Phi(\mathbf{k}_4) \rangle \\ &= (2\pi)^3 \delta^D(\mathbf{k}_1 + \mathbf{k}_2 + \mathbf{k}_3 + \mathbf{k}_4) \\ &\times \left\{ \frac{25}{18} \tau_{\text{NL}} [P_\Phi(k_1) P_\Phi(k_2) \{P_\Phi(k_{13}) + P_\Phi(k_{14})\} + (11 \text{ perm.})] \right. \\ &\quad \left. + 6g_{\text{NL}} [P_\Phi(k_1) P_\Phi(k_2) P_\Phi(k_3) + (3 \text{ perm.})] \right\}, \end{aligned} \quad (63)$$

* The CMB bispectrum from the second-order ISW effect was considered in [133].

‡ Incidentally, in the notation of [121] (see their equation 2.29), $S_{00}^{(2)}(\mathbf{k}', \mathbf{k}'', \mathbf{k}, \eta_*) = \frac{4}{3} R_* \left(\frac{k'k''\eta_*}{k} \right)^2 F_2^{(s)}(\mathbf{k}', \mathbf{k}'') T(k') T(k'')$.

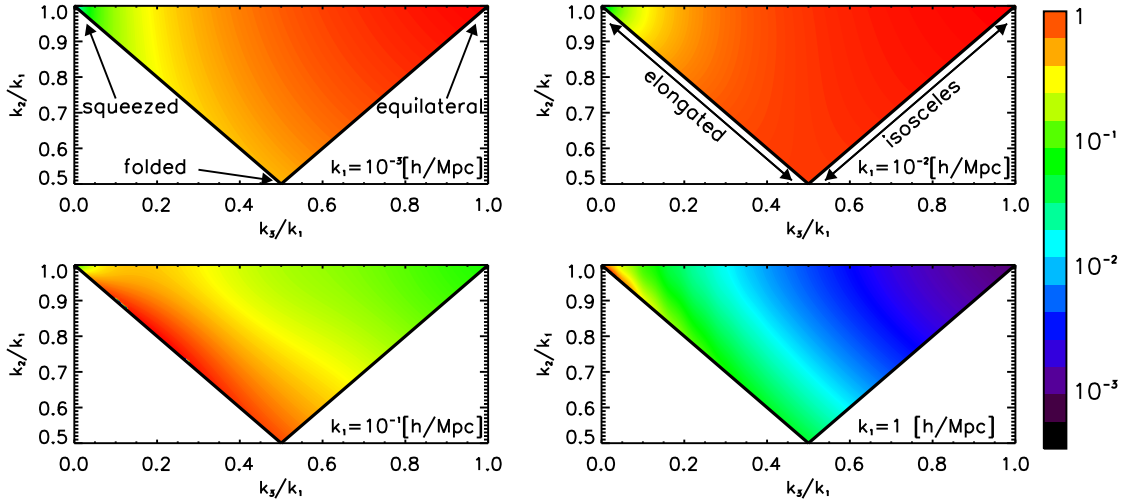


Figure 4. Shapes of the second-order bispectrum due to the second-order curvature perturbations in the Newtonian limit given in equation 60. Each panel shows the normalized amplitude of $F_{2\text{nd}}(k_1, k_2, k_3)(k_2/k_1)^2(k_3/k_1)^2$ as a function of k_2/k_1 and k_3/k_1 for a given k_1 , with a condition that $k_3 \leq k_2 \leq k_1$ is satisfied. The amplitude is normalized such that it is unity at the point where $F_{2\text{nd}}(k_1, k_2, k_3)(k_2/k_1)^2(k_3/k_1)^2$ takes on the maximum value. (Top Left) $k_1 = 10^{-3} h \text{ Mpc}^{-1}$. (Top Right) $k_1 = 10^{-2} h \text{ Mpc}^{-1}$. (Bottom Left) $k_1 = 10^{-1} h \text{ Mpc}^{-1}$. (Bottom Right) $k_1 = 1 h \text{ Mpc}^{-1}$. The CMB data are sensitive to $k_1 < k_{\text{max}} \sim 0.2 h \text{ Mpc}^{-1}(l_{\text{max}}/2000)$, where the second-order bispectrum peaks at the equilateral configuration on large scales, and peaks along the elongated configurations on a smaller scale ($k_1 \sim 0.1 h \text{ Mpc}^{-1}$). On a very small scale ($k_1 \sim 1 h \text{ Mpc}^{-1}$), it peaks at the squeezed configuration. Note that the most squeezed configuration shown here has $k_1 = k_2 = 100k_3$.

where $k_{ij} \equiv |\mathbf{k}_i + \mathbf{k}_j|$. (In this section, we use Φ for the primordial perturbation, i.e., $\Phi = \Phi_p = \frac{3}{5}\zeta$.) When the curvature perturbation is given by the simplest local form, $\Phi = \Phi_L + f_{\text{NL}}^{\text{local}}\Phi_L^2 + g_{\text{NL}}\Phi_L^3$, one finds the above trispectrum with $\tau_{NL} = (6f_{\text{NL}}^{\text{local}}/5)^2$ [43]. However, in general τ_{NL} is different from $(6f_{\text{NL}}^{\text{local}}/5)^2$.

To see this, let us consider a broad class of multi-field models in which the primordial curvature perturbation, ζ , is given in terms of the field derivatives of the number of e -folds, $N = \ln a$, and the perturbation in the I -th scalar field, $\delta\phi_I$, as

$$\zeta = \sum_I \frac{\partial N}{\partial \phi_I} \delta\phi_I + \frac{1}{2} \sum_{IJ} \frac{\partial^2 N}{\partial \phi_I \partial \phi_J} \delta\phi_I \delta\phi_J + \dots, \quad (64)$$

where $\langle \delta\phi_I \delta\phi_J \rangle = 0$ for $I \neq J$. This expansion is known as the “ δN formalism” [22, 82, 108, 135, 136]. In this case, $f_{\text{NL}}^{\text{local}}$ and τ_{NL} are given by [22, 45]

$$\frac{6}{5}f_{\text{NL}}^{\text{local}} = \frac{\sum_{IJ} N_{,IJ} N_{,I} N_{,J}}{[\sum_I (N_{,I})^2]^2}, \quad (65)$$

$$\tau_{NL} = \frac{\sum_{IJK} N_{,IJ} N_{,J} N_{,IK} N_{,K}}{[\sum_I (N_{,I})^2]^3} = \frac{\sum_I (\sum_J N_{,IJ} N_{,J})^2}{[\sum_I (N_{,I})^2]^3}, \quad (66)$$

where $N_{,I} \equiv \partial N / \partial \phi_I$ and $N_{,IJ} \equiv \partial^2 N / \partial \phi_I \partial \phi_J$. Suyama and Yamaguchi [48] showed

that the Cauchy-Schwarz inequality implies that the following inequality,

$$\tau_{\text{NL}} \geq \left(\frac{6f_{\text{NL}}^{\text{local}}}{5} \right)^2, \quad (67)$$

is satisfied. To derive this result, use the Cauchy-Schwarz inequality:

$$\left(\sum_I a_I^2 \right) \left(\sum_J b_J^2 \right) \geq \left(\sum_I a_I b_I \right)^2, \quad (68)$$

with

$$a_I = \frac{\sum_J N_{IJ} N_{J,I}}{[\sum_J (N_{J,I})^2]^{3/2}}, \quad (69)$$

$$b_I = \frac{N_{I,I}}{[\sum_J (N_{J,I})^2]^{1/2}}. \quad (70)$$

Note, however, that one finds a different relation between $f_{\text{NL}}^{\text{local}}$ and τ_{NL} when the Cauchy-Schwarz inequality becomes trivial, i.e., $0 = 0$. For example, when ζ is given by [43]

$$\zeta = \frac{\partial N}{\partial \phi_1} \delta \phi_1 + \frac{1}{2} \frac{\partial^2 N}{\partial \phi_2^2} \delta \phi_2^2, \quad (71)$$

and $\langle \delta \phi_1 \delta \phi_2 \rangle = 0$, one finds $\tau_{\text{NL}} \sim 10^3 (f_{\text{NL}}^{\text{local}})^{4/3}$ [49]. The Cauchy-Schwarz inequality becomes $0 = 0$ because $a_I = 0$ for all I . In this case, whether $\tau_{\text{NL}} \geq (6f_{\text{NL}}^{\text{local}}/5)^2$ is satisfied depends on the value of $f_{\text{NL}}^{\text{local}}$. For this particular example, the current limit of $f_{\text{NL}}^{\text{local}} < 74$ implies that $\tau_{\text{NL}} \geq (6f_{\text{NL}}^{\text{local}}/5)^2$ is still satisfied parametrically.

Therefore, if observations indicate $\tau_{\text{NL}} < (6f_{\text{NL}}^{\text{local}}/5)^2$, a broad class of multi-field models satisfying the above conditions would be ruled out. This property makes the trispectrum a powerful probe of the physics of multi-field models.

The expected 95% uncertainties in τ_{NL} from the 7-year *WMAP* data ($l_{\text{max}} \sim 500$) and the 1-year *Planck* data ($l_{\text{max}} \sim 1500$) are 5000 and 560, respectively [67]. *If the Planck finds $f_{\text{NL}}^{\text{local}} \sim 30$, then it would be able to test if the measured τ_{NL} would satisfy equation 67.* This provides an excellent science case for the trispectrum that would be measured by *Planck*.

The expected uncertainties in g_{NL} have not been calculated yet, although we expect them to be much greater than those for τ_{NL} , as g_{NL} is the coefficient of the cubic-order term (i.e., g_{NL} is much more difficult to constrain than τ_{NL}) [137].

The local-form trispectrum is not the only possibility. Various other inflation models predict distinctly different quadrilateral shape dependence. For some general analyses of shapes, see [34, 41, 55, 63].

Finally, while we do not discuss the large-scale structure of the universe in this article, the most promising probe of the local-form trispectrum seems to be the *bispectrum* of galaxies. See [80, 138, 139] for details.

Band	Foreground	$f_{\text{NL}}^{\text{local}}$	$f_{\text{NL}}^{\text{equil}}$	$f_{\text{NL}}^{\text{orthog}}$	b_{src}
V+W	Raw	59 ± 21	33 ± 140	-199 ± 104	N/A
V+W	Clean	42 ± 21	29 ± 140	-198 ± 104	N/A
V+W	Marg.	32 ± 21	26 ± 140	-202 ± 104	-0.08 ± 0.12
V	Marg.	43 ± 24	64 ± 150	-98 ± 115	0.32 ± 0.23
W	Marg.	39 ± 24	36 ± 154	-257 ± 117	-0.13 ± 0.19

Table 1. Estimates and the corresponding 68% intervals of the primordial non-Gaussianity parameters ($f_{\text{NL}}^{\text{local}}$, $f_{\text{NL}}^{\text{equil}}$, $f_{\text{NL}}^{\text{orthog}}$) and the point source bispectrum amplitude, b_{src} (in units of $10^{-5} \mu\text{K}^3 \text{sr}^2$), from the *WMAP* 7-year temperature maps. This table is adopted from [11].

7. Current Results

7.1. Bispectrum

(Most of this subsection is adopted from Section 6.2 of [11].)

In 2002, the first limit on $f_{\text{NL}}^{\text{local}}$ was obtained from the *COBE* 4-year data [140] by [141], using the angular bispectrum. The limit was improved by an order of magnitude when the *WMAP* first year data were used to constrain $f_{\text{NL}}^{\text{local}}$ [142]. Since then the limits have improved steadily as *WMAP* collects more years of data and the bispectrum method for estimating $f_{\text{NL}}^{\text{local}}$ has improved [6, 7, 10, 79, 143–147].

Using the optimal estimators described in Section 3, we have constrained the primordial non-Gaussianity parameters as well as the point-source bispectrum using the *WMAP* 7-year data. The 7-year data and results are described in Refs. [11, 71, 148–151].

We use the V- and W-band maps at the HEALPix resolution $N_{\text{side}} = 1024$. As the optimal estimator weights the data optimally at all multipoles, we no longer need to choose the maximum multipole used in the analysis, i.e., we use all the data. We use both the raw maps (before cleaning foreground) and foreground-reduced (clean) maps to quantify the foreground contamination of f_{NL} parameters. For all cases, we find the best limits on f_{NL} parameters by combining the V- and W-band maps, and marginalizing over the synchrotron, free-free, and dust foreground templates [149]. As for the mask, we always use the *KQ75y7* mask [149].

In Table 7.1, we summarize our results:

1. **Local form results.** The 7-year best estimate of $f_{\text{NL}}^{\text{local}}$ is

$$f_{\text{NL}}^{\text{local}} = 32 \pm 21 \text{ (68\% CL).}$$

The 95% limit is $-10 < f_{\text{NL}}^{\text{local}} < 74$. When the raw maps are used, we find $f_{\text{NL}}^{\text{local}} = 59 \pm 21$ (68% CL). When the clean maps are used, but foreground templates are not marginalized over, we find $f_{\text{NL}}^{\text{local}} = 42 \pm 21$ (68% CL). These results (in particular the clean-map versus the foreground marginalized) indicate that the

foreground emission makes a difference at the level of $\Delta f_{\text{NL}}^{\text{local}} \sim 10$.^{††} We find that the V+W result is lower than the V-band or W-band results. This is possible, as the V+W result contains contributions from the cross-correlations of V and W such as $\langle VVW \rangle$ and $\langle VWV \rangle$.

2. Equilateral form results. The 7-year best estimate of $f_{\text{NL}}^{\text{equil}}$ is

$$f_{\text{NL}}^{\text{equil}} = 26 \pm 140 \text{ (68\% CL).}$$

The 95% limit is $-214 < f_{\text{NL}}^{\text{equil}} < 266$. For $f_{\text{NL}}^{\text{equil}}$, the foreground marginalization does not shift the central values very much, $\Delta f_{\text{NL}}^{\text{equil}} = -3$. This makes sense, as the equilateral bispectrum does not couple small-scale modes to very large-scale modes $l < 10$, which are sensitive to the foreground emission. On the other hand, the local form bispectrum is dominated by the squeezed triangles, which do couple large and small scales modes.

3. Orthogonal form results. The 7-year best estimate of $f_{\text{NL}}^{\text{orthog}}$ is

$$f_{\text{NL}}^{\text{orthog}} = -202 \pm 104 \text{ (68\% CL).}$$

The 95% limit is $-410 < f_{\text{NL}}^{\text{orthog}} < 6$. The foreground marginalization has little effect, $\Delta f_{\text{NL}}^{\text{orthog}} = -4$.

As for the point-source bispectrum, we do not detect b_{src} in V, W, or V+W. In [79], we estimated that the residual sources could bias $f_{\text{NL}}^{\text{local}}$ by a small positive amount, and applied corrections using Monte Carlo simulations. In this paper, we do not attempt to make such corrections, but we note that sources could give $\Delta f_{\text{NL}}^{\text{local}} \sim 2$ (note that the simulations used by [79] likely overestimated the effect of sources by a factor of two). As the estimator has changed from that used by [79], extrapolating the previous results is not trivial. Source corrections to $f_{\text{NL}}^{\text{equil}}$ and $f_{\text{NL}}^{\text{orthog}}$ could be larger [79], but we have not estimated the magnitude of the effect for the 7-year data.

As we described in Section 4, among various sources of secondary non-Gaussianities which might contaminate measurements of primordial non-Gaussianity (in particular $f_{\text{NL}}^{\text{local}}$), a coupling between the ISW effect and the weak gravitational lensing is the most dominant source of confusion for $f_{\text{NL}}^{\text{local}}$. Calabrese et al. [153] used the skewness power spectrum method of [154] to search for this term in the *WMAP* 5-year data and found a null result.

7.2. Trispectrum

The optimal estimators for the trispectrum have not been implemented, largely because they are computationally demanding. While the first measurements of the angular

^{††}The effect of the foreground marginalization depends on an estimator. Using the needlet bispectrum, Cabella et al. [152] found $f_{\text{NL}}^{\text{local}} = 35 \pm 42$ and 38 ± 47 (68% CL) with and without the foreground marginalization, respectively.

bispectrum were made from the the *COBE* 4-year data [140] by [1, 155] in 2001, limits on the physical parameters have not been obtained from the direct trispectrum analysis.

Recently, Smidtu et al. [69] used the sub-optimal estimator developed in [156] (which becomes optimal in the limit that the instrumental noise is isotropic) and found the 95% CL limits of $-3.8 \times 10^6 < g_{\text{NL}} < 3.9 \times 10^6$ and $-3.2 \times 10^5 < \tau_{\text{NL}} < 3.3 \times 10^5$. The uncertainty in τ_{NL} is about 70 times larger than expected [67], and thus there is a large room for improvement with the optimal estimator. The current limit is consistent with the Suyama-Yamaguchi inequality, $\tau_{\text{NL}} \geq (6f_{\text{NL}}^{\text{local}}/5)^2$.

7.3. Other statistical methods

While the optimal estimators for the f_{NL} parameters (with the minimum variance) must be constructed from the PDF as in Section 3, there are various other ways of constraining non-Gaussianity. While these other methods are usually sub-optimal, they serve as useful diagnosis tools of the results obtained from the direct bispectrum and trispectrum methods. In some cases, they are easier to implement than the optimal estimators.

A major progress in the topological Gaussianity test using the *Minkowski functionals* [157–161] since 2004 is the derivation and implementation of the analytical formula for the Minkowski functionals of the CMB [162, 163]. This method has been applied to the *WMAP* data [164, 165] as well as to the BOOMERanG data [166]. The *Planck* data are expected to reach the 68% limit of $\Delta f_{\text{NL}}^{\text{local}} = 20$ [162], which is worse than the limit from the optimal method, $\Delta f_{\text{NL}}^{\text{local}} = 5$ [76]. An advantage of the Minkowski functionals is that the measurements of the Minkowski functionals do not depend on the models, and thus the computational cost is the same for all models. This allows one to obtain limits on various models, for which the optimal estimators are difficult to implement. For example, a limit on the primordial non-Gaussianity in the isocurvature perturbation is currently available only from the Minkowski functionals [165].

Instead of expanding the temperature anisotropy into spherical harmonics, one may choose to expand it using a different basis. One popular basis used in the CMB community is the so-called *Spherical Mexican Hat Wavelet* (SMHW). See [167, 168] for reviews on this method. A major progress in this method is the realization that the 3-point function of the wavelet coefficients made of large and small smoothing scales is nearly an optimal estimator for the local-form bispectrum: when only the adjacent scales are included, Curto et al. [169] found $-8 < f_{\text{NL}}^{\text{local}} < 111$ (95% CL) from the *WMAP* 5-year data. When all the scales (including large-small scale combinations) are included in the analysis, the limit improved significantly to $-18 < f_{\text{NL}}^{\text{local}} < 80$ (95% CL) [170], which is similar to the optimal limit from the 5-year data, $-4 < f_{\text{NL}}^{\text{local}} < 80$ (95% CL) [10]. An advantage of the SMHW is that it retains information on the spatial distribution of the signal. This property can be used to measure $f_{\text{NL}}^{\text{local}}$ as a function of positions on the sky [170]. In addition, the analytical formula for the SMHW as a function of $f_{\text{NL}}^{\text{local}}$ has been derived and implemented (A. Curto 2009, private communication). See [171, 172]

for earlier limits on $f_{\text{NL}}^{\text{local}}$ from the SMHW.

Another form of spherical wavelets that has been used to constrain $f_{\text{NL}}^{\text{local}}$ is the *spherical needlets* [173]. The limits on $f_{\text{NL}}^{\text{local}}$ are reported in [152, 174, 175]. This method also allows one to look for a spatial variation in $f_{\text{NL}}^{\text{local}}$, and the results are reported in [176, 177]. For the other types of wavelets considered in the literature, see [178, 179] and references therein.

Many other statistical methods have been proposed and used for constraining $f_{\text{NL}}^{\text{local}}$ in the literature. An incomplete list of references is: [180, 181] on the real-space 3-point function; [182] on the integrated bispectrum; [183] on the 2-1 cumulant correlator; [172] on the local curvature; and [68, 184] on the N -point PDF. Also see references therein. While we have not listed the statistical methods that have not been used to constrain the primordial non-Gaussianity parameters yet, there are many other methods proposed in a general context in the literature.

8. Conclusion

Since the last review articles on signatures of primordial non-Gaussianity in the CMB were written in 2001 [1] and 2004 [2], a lot of progress has been made in this field. The current standard lore may be summarized as follows:

1. **Shape and physics.** Different aspects of the physics of the primordial universe appear in different shapes of three- and four-point functions.
2. **Importance of local shape.** Of these shapes, the local shapes have special significance: a significant detection of the local-form bispectrum (with $f_{\text{NL}}^{\text{local}} \gg 1$) would rule out *all* single-field inflation models, and the local-form trispectrum can be used to rule out a broad class of multi-field models by testing $\tau_{\text{NL}} \geq (6f_{\text{NL}}^{\text{local}}/5)^2$.
3. **Optimal estimators.** The optimal estimators of the bispectrum and trispectrum can be derived systematically from the expansion of the PDF. The optimal bispectrum estimator has been implemented.
4. **Secondary.** The most serious contamination of $f_{\text{NL}}^{\text{local}}$ is due to the lensing-ISW coupling, which can be removed by using the template given in Section 4.
5. **Foreground.** The Galactic foreground contamination is minimal for $f_{\text{NL}}^{\text{equil}}$ and $f_{\text{NL}}^{\text{orthog}}$, but it can be as large as $f_{\text{NL}}^{\text{local}} \sim 10$ for the local-form bispectrum. This must be carefully studied and eliminated in the *Planck* data analysis. The random (Poisson) point-source contamination can be removed by using the template given in Section 3.2.

Some outstanding issues for the “CMB and primordial non-Gaussianity” include:

1. **Second order.** (In Newtonian gauge) the products of the first-order terms and the intrinsically second-order terms in the sub-horizon limit do not contaminate the local-form bispectrum very much ($\Delta f_{\text{NL}}^{\text{local}} < 1$). However, would the post-Newtonian effect give $\Delta f_{\text{NL}}^{\text{local}} \sim 5$, as found by [131]? If so, we need to construct a template for this effect.

2. **More foreground.** How can we model the non-Poisson (clustered) point source bispectrum? How about the foreground (and secondary) contamination of the primordial trispectrum?
3. **Trispectrum estimators.** How can we implement the optimal trispectrum estimators for both local and non-local shapes?

These issues would become important when the *Planck* data are analyzed in search of primordial non-Gaussianity. The *Planck* is expected to reduce the uncertainty in $f_{\text{NL}}^{\text{local}}$ by a factor of four compared to the current limit, $f_{\text{NL}}^{\text{local}} = 32 \pm 21$ (68% CL). If the *Planck* detected $f_{\text{NL}}^{\text{local}} \sim 30$, then the trispectrum would provide an important test of multi-field models.

However, do not despair even if the *Planck* did not detect the primordial bispectrum or trispectrum - while the CMB may end its leading role as a probe of primordial non-Gaussianity (unless the next-generation, comprehensive CMB satellite which can measure both the temperature and polarization to the cosmic-variance-limited precision is funded [185]), the large-scale structure of the universe would eventually take over and substantially reduce the uncertainties in the local-form parameters such as $f_{\text{NL}}^{\text{local}}$, τ_{NL} , and g_{NL} (see Desjacques and Seljak's article in this volume).

Acknowledgments

We thank the organizers and participants of “The Non-Gaussian Universe” workshop at Yukawa Institute for Theoretical Physics (YITP) for stimulating discussion and presentations, D. Jeong for making Figure 3 and 4, D. Nitta for calculating $f_{\text{NL}}^{\text{local}}$ from the second-order Φ in the Newtonian limit, and T. Takahashi for valuable comments on Section 6. This work is supported in part by an NSF grant PHY-0758153.

References

- [1] Komatsu E 2001 Ph.D. thesis at Tohoku University (astro-ph/0206039)
- [2] Bartolo N, Komatsu E, Matarrese S and Riotto A 2004 *Phys. Rept.* **402** 103–266 (*Preprint* astro-ph/0406398)
- [3] Maldacena J M 2003 *JHEP* **05** 013 (*Preprint* astro-ph/0210603)
- [4] Acquaviva V, Bartolo N, Matarrese S and Riotto A 2003 *Nucl. Phys.* **B667** 119–148 (*Preprint* astro-ph/0209156)
- [5] Creminelli P and Zaldarriaga M 2004 *Journal of Cosmology and Astro-Particle Physics* **10** 6–+ (*Preprint* arXiv:astro-ph/0407059)
- [6] Komatsu E, Spergel D N and Wandelt B D 2005 *Astrophys. J.* **634** 14–19
- [7] Creminelli P, Nicolis A, Senatore L, Tegmark M and Zaldarriaga M 2006 *JCAP* **0605** 004 (*Preprint* astro-ph/0509029)
- [8] Smith K M and Zaldarriaga M 2006 *ArXiv e-prints*, astro-ph/0612571 (*Preprint* astro-ph/0612571)

- [9] Yadav A P S, Komatsu E, Wandelt B D, Liguori M, Hansen F K and Matarrese S 2008 *Astrophys. J.* **678** 578–582 (*Preprint arXiv:0711.4933*)
- [10] Smith K M, Senatore L and Zaldarriaga M 2009 *Journal of Cosmology and Astroparticle Physics* **9** 6–+ (*Preprint 0901.2572*)
- [11] Komatsu E *et al.* 2010 *Astrophys. J. Suppl.*, submitted (*Preprint 1001.4538*)
- [12] Goldberg D M and Spergel D N 1999 *Phys. Rev. D* **59** 103002
- [13] Verde L and Spergel D N 2002 *Phys. Rev. D* **65** 043007 (*Preprint astro-ph/0108179*)
- [14] Serra P and Cooray A 2008 *Phys. Rev. D* **77** 107305 (*Preprint 0801.3276*)
- [15] Hanson D, Smith K M, Challinor A and Liguori M 2009 *Phys. Rev. D* **80**(8) 083004–+ (*Preprint 0905.4732*)
- [16] Mangilli A and Verde L 2009 *Phys. Rev. D* **80**(12) 123007–+ (*Preprint 0906.2317*)
- [17] Creminelli P 2003 *JCAP* **0310** 003 (*Preprint astro-ph/0306122*)
- [18] Babich D, Creminelli P and Zaldarriaga M 2004 *JCAP* **0408** 009 (*Preprint astro-ph/0405356*)
- [19] Chen X, Huang M x, Kachru S and Shiu G 2007 *JCAP* **0701** 002 (*Preprint hep-th/0605045*)
- [20] Lyth D H, Ungarelli C and Wands D 2003 *Phys. Rev. D* **67** 23503
- [21] Zaldarriaga M 2004 *Phys. Rev. D* **69** 043508 (*Preprint astro-ph/0306006*)
- [22] Lyth D H and Rodriguez Y 2005 *Phys. Rev. Lett.* **95** 121302 (*Preprint astro-ph/0504045*)
- [23] Lehners J 2008 *Phys. Rep.* **465** 223–263 (*Preprint 0806.1245*)
- [24] Bond J R, Frolov A V, Huang Z and Kofman L 2009 *Physical Review Letters* **103**(7) 071301–+ (*Preprint 0903.3407*)
- [25] Chambers A, Nurmi S and Rajantie A 2010 *JCAP* **1001** 012 (*Preprint 0909.4535*)
- [26] Alishahiha M, Silverstein E and Tong D 2004 *Phys. Rev. D* **70**(12) 123505–+ (*Preprint arXiv:hep-th/0404084*)
- [27] Arkani-Hamed N, Creminelli P, Mukohyama S and Zaldarriaga M 2004 *JCAP* **0404** 001 (*Preprint hep-th/0312100*)
- [28] Seery D and Lidsey J E 2005 *JCAP* **0506** 003 (*Preprint astro-ph/0503692*)
- [29] Holman R and Tolley A J 2008 *JCAP* **0805** 001 (*Preprint 0710.1302*)
- [30] Meerburg P D, van der Schaar J P and Corasaniti P S 2009 *JCAP* **0905** 018 (*Preprint 0901.4044*)
- [31] Senatore L, Smith K M and Zaldarriaga M 2010 *Journal of Cosmology and Astroparticle Physics* **1** 28–+ (*Preprint 0905.3746*)
- [32] Moss I G and Xiong C 2007 *JCAP* **0704** 007 (*Preprint astro-ph/0701302*)
- [33] Arroja F, Mizuno S and Koyama K 2008 *JCAP* **0808** 015 (*Preprint 0806.0619*)
- [34] Renaux-Petel S 2009 *JCAP* **0910** 012 (*Preprint 0907.2476*)

- [35] Meerburg P D, van der Schaar J P and Jackson M G 2010 *JCAP* **1002** 001 (*Preprint* 0910.4986)
- [36] Chen X and Wang Y 2009 *ArXiv e-prints*, *arXiv:0909.0496* (*Preprint* 0909.0496)
- [37] Chen X, Easter R and Lim E A 2007 *JCAP* **0706** 023 (*Preprint* astro-ph/0611645)
- [38] Chen X, Easter R and Lim E A 2008 *JCAP* **0804** 010 (*Preprint* 0801.3295)
- [39] Arroja F and Koyama K 2008 *Phys. Rev.* **D77** 083517 (*Preprint* 0802.1167)
- [40] Arroja F, Mizuno S, Koyama K and Tanaka T 2009 *Phys. Rev.* **D80** 043527 (*Preprint* 0905.3641)
- [41] Chen X, Hu B, Huang M x, Shiu G and Wang Y 2009 *JCAP* **0908** 008 (*Preprint* 0905.3494)
- [42] Seery D, Sloth M S and Vernizzi F 2009 *JCAP* **0903** 018 (*Preprint* 0811.3934)
- [43] Boubekeur L and Lyth D H 2006 *Phys. Rev. D* **73**(2) 021301–+ (*Preprint* arXiv:astro-ph/0504046)
- [44] Huang M X and Shiu G 2006 *Phys. Rev. D* **74**(12) 121301–+ (*Preprint* arXiv:hep-th/0610235)
- [45] Byrnes C T, Sasaki M and Wands D 2006 *Phys. Rev. D* **74**(12) 123519–+ (*Preprint* arXiv:astro-ph/0611075)
- [46] Seery D and Lidsey J E 2007 *JCAP* **0701** 008 (*Preprint* astro-ph/0611034)
- [47] Seery D, Lidsey J E and Sloth M S 2007 *JCAP* **0701** 027 (*Preprint* astro-ph/0610210)
- [48] Suyama T and Yamaguchi M 2008 *Phys. Rev.* **D77** 023505 (*Preprint* 0709.2545)
- [49] Suyama T and Takahashi F 2008 *Journal of Cosmology and Astro-Particle Physics* **9** 7–+ (*Preprint* 0804.0425)
- [50] Ichikawa K, Suyama T, Takahashi T and Yamaguchi M 2008 *Phys. Rev.* **D78** 023513 (*Preprint* 0802.4138)
- [51] Ichikawa K, Suyama T, Takahashi T and Yamaguchi M 2008 *Phys. Rev.* **D78** 063545 (*Preprint* 0807.3988)
- [52] Buchbinder E I, Khoury J and Ovrut B A 2008 *Phys. Rev. Lett.* **100** 171302 (*Preprint* 0710.5172)
- [53] Mizuno S, Arroja F, Koyama K and Tanaka T 2009 *Phys. Rev.* **D80** 023530 (*Preprint* 0905.4557)
- [54] Mizuno S, Arroja F and Koyama K 2009 *Phys. Rev.* **D80** 083517 (*Preprint* 0907.2439)
- [55] Gao X, Li M and Lin C 2009 *JCAP* **0911** 007 (*Preprint* 0906.1345)
- [56] Gao X and Hu B 2009 *JCAP* **0908** 012 (*Preprint* 0903.1920)
- [57] Byrnes C T, Choi K Y and Hall L M H 2009 *JCAP* **0902** 017 (*Preprint* 0812.0807)
- [58] Byrnes C T and Tasinato G 2009 *JCAP* **0908** 016 (*Preprint* 0906.0767)

- [59] Enqvist K and Takahashi T 2008 *Journal of Cosmology and Astro-Particle Physics* **9** 12–+ (*Preprint* 0807.3069)
- [60] Enqvist K, Nurmi S, Taanila O and Takahashi T 2009 *ArXiv e-prints* (*Preprint* 0912.4657)
- [61] Enqvist K and Takahashi T 2009 *Journal of Cosmology and Astro-Particle Physics* **12** 1–+ (*Preprint* 0909.5362)
- [62] Kawasaki M, Takahashi T and Yokoyama S 2009 *Journal of Cosmology and Astro-Particle Physics* **12** 12–+ (*Preprint* 0910.3053)
- [63] Chen X and Wang Y 2009 *ArXiv e-prints, arXiv:0911.3380* (*Preprint* 0911.3380)
- [64] Kawakami E, Kawasaki M, Nakayama K and Takahashi F 2009 *JCAP* **0909** 002 (*Preprint* 0905.1552)
- [65] Takahashi T, Yamaguchi M and Yokoyama S 2009 *Phys. Rev. D* **80**(6) 063524–+ (*Preprint* 0907.3052)
- [66] Okamoto T and Hu W 2002 *Phys. Rev. D* **66**(6) 063008–+ (*Preprint* arXiv:astro-ph/0206155)
- [67] Kogo N and Komatsu E 2006 *Phys. Rev. D* **73** 083007 (*Preprint* astro-ph/0602099)
- [68] Vielva P and Sanz J L 2009 (*Preprint* 0910.3196)
- [69] Smidt J *et al.* 2010 (*Preprint* 1001.5026)
- [70] Komatsu E *et al.* 2009 *Astro2010: The Astronomy and Astrophysics Decadal Survey, Science White Papers, no. 158* (*arXiv:0902.4759*)
- [71] Larson D *et al.* 2010 *Astrophys. J. Suppl.*, submitted (*Preprint* 1001.4635)
- [72] Reichardt C L, Ade P A R, Bock J J, Bond J R, Brevik J A, Contaldi C R, Daub M D, Dempsey J T, Goldstein J H, Holzapfel W L, Kuo C L, Lange A E, Lueker M, Newcomb M, Peterson J B, Ruhl J, Runyan M C and Staniszewski Z 2009 *Astrophys. J.* **694** 1200–1219 (*Preprint* 0801.1491)
- [73] Brown M L, Ade P, Bock J, Bowden M, Cahill G, Castro P G, Church S, Culverhouse T, Friedman R B, Ganga K, Gear W K, Gupta S, Hinderks J, Kovac J, Lange A E, Leitch E, Melhuish S J, Memari Y, Murphy J A, Orlando A, O’Sullivan C, Piccirillo L, Pryke C, Rajguru N, Rusholme B, Schwarz R, Taylor A N, Thompson K L, Turner A H, Wu E Y S, Zemcov M and The QUA D collaboration 2009 *Astrophys. J.* **705** 978–999 (*Preprint* 0906.1003)
- [74] Taylor A and Watts P 2001 *Mon. Not. Roy. Astron. Soc.* **328** 1027 (*Preprint* astro-ph/0010014)
- [75] Babich D 2005 *Phys. Rev. D* **72** 043003 (*Preprint* astro-ph/0503375)
- [76] Komatsu E and Spergel D N 2001 *Phys. Rev. D* **63** 063002 (*Preprint* astro-ph/0005036)
- [77] Hu W 2000 *Phys. Rev. D* **62** 43007–+

- [78] Gorski K M, Hivon E, Banday A J, Wandelt B D, Hansen F K, Reinecke M and Bartlemann M 2005 *Astrophys. J.* **622** 759 (*Preprint astro-ph/0409513*)
- [79] Komatsu E, Dunkley J, Nolta M R, Bennett C L, Gold B, Hinshaw G, Jarosik N, Larson D, Limon M, Page L, Spergel D N, Halpern M, Hill R S, Kogut A, Meyer S S, Tucker G S, Weiland J L, Wollack E and Wright E L 2009 *Astrophys. J. Suppl.* **180** 330–376 (*Preprint 0803.0547*)
- [80] Jeong D and Komatsu E 2009 *Astrophys. J.* **691** 569–595 (*Preprint 0805.2632*)
- [81] Starobinskii A A 1979 *Soviet Journal of Experimental and Theoretical Physics Letters* **30** 682–+
- [82] Starobinsky A A 1982 *Phys. Lett.* **B117** 175–178
- [83] Guth A H 1981 *Phys. Rev. D* **23** 347
- [84] Sato K 1981 *Mon. Not. R. Astr. Soc.* **195** 467–479
- [85] Linde A D 1982 *Phys. Lett.* **B108** 389–393
- [86] Albrecht A and Steinhardt P J 1982 *Phys. Rev. Lett.* **48** 1220–1223
- [87] Mukhanov V F and Chibisov G V 1981 *JETP Letters* **33** 532
- [88] Hawking S W 1982 *Phys. Lett.* **B115** 295
- [89] Guth A H and Pi S Y 1982 *Phys. Rev. Lett.* **49** 1110–1113
- [90] Bardeen J M, Steinhardt P J and Turner M S 1983 *Phys. Rev. D* **28** 679
- [91] Linde A D 1990 *Particle physics and inflationary cosmology* (Chur, Switzerland: Harwood)
- [92] Mukhanov V F, Feldman H A and Brandenberger R H 1992 *Phys. Rept.* **215** 203–333
- [93] Liddle A R and Lyth D H 2000 *Cosmological inflation and large-scale structure* (Cambridge University Press)
- [94] Liddle A R and Lyth D H 2009 *The Primordial Density Perturbation: Cosmology, Inflation and the Origin of Structure* (Cambridge University Press)
- [95] Bassett B A, Tsujikawa S and Wands D 2006 *Rev. Mod. Phys.* **78** 537–589 (*Preprint astro-ph/0507632*)
- [96] Linde A 2008 *Lect. Notes Phys.* **738** 1–54 (*Preprint arXiv:0705.0164[hep-th]*)
- [97] Bardeen J M 1980 *Phys. Rev. D* **22** 1882–1905
- [98] Kodama H and Sasaki M 1984 *Prog. Theor. Phys. Suppl.* **78** 1–166
- [99] Sachs R K and Wolfe A M 1967 *Astrophys. J.* **147** 73
- [100] Gangui A, Lucchin F, Matarrese S and Mollerach S 1994 *Astrophys. J.* **430** 447–457
- [101] Verde L, Wang L, Heavens A F and Kamionkowski M 2000 *Mon. Not. R. Astr. Soc.* **313** 141–147 (*Preprint arXiv:astro-ph/9906301*)
- [102] Linde A and Mukhanov V 1997 *Phys. Rev. D* **56** 535–539
- [103] Dvali G, Gruzinov A and Zaldarriaga M 2004 *Phys. Rev. D* **69**(8) 083505–+

- [104] Dvali G, Gruzinov A and Zaldarriaga M 2004 *Phys. Rev. D* **69**(2) 023505–+
- [105] Enqvist K, Jokinen A, Mazumdar A, Multamäki T and Väihkönen A 2005 *Phys. Rev. Lett.* **94**(16) 161301–+ (*Preprint arXiv:astro-ph/0411394*)
- [106] Jokinen A and Mazumdar A 2006 *JCAP* **0604** 003 (*Preprint astro-ph/0512368*)
- [107] Chambers A and Rajantie A 2008 *Phys. Rev. Lett.* **100** 041302 (*Preprint arXiv:0710.4133[astro-ph]*)
- [108] Salopek D S and Bond J R 1990 *Phys. Rev. D* **42** 3936–3962
- [109] Falk T, Rangarajan R and Srednicki M 1993 *Astrophys. J. Lett.* **403** L1–L3
- [110] Silverstein E and Tong D 2004 *Phys. Rev. D* **70**(10) 103505–+ (*Preprint arXiv:hep-th/0310221*)
- [111] Cheung C, Creminelli P, Fitzpatrick A L, Kaplan J and Senatore L 2008 *JHEP* **03** 014 (*Preprint 0709.0293*)
- [112] Li M, Wang T and Wang Y 2008 *JCAP* **0803** 028 (*Preprint 0801.0040*)
- [113] Moss I G and Graham C M 2007 *JCAP* **0711** 004 (*Preprint arXiv:0707.1647[astro-ph]*)
- [114] Seljak U and Zaldarriaga M 1996 *Astrophys. J.* **469** 437
- [115] Lewis A, Challinor A and Lasenby A 2000 *Astrophys. J.* **538** 473–476
- [116] Babich D and Zaldarriaga M 2004 *Phys. Rev. D* **70** 083005 (*Preprint astro-ph/0408455*)
- [117] Yadav A P S, Komatsu E and Wandelt B D 2007 *Astrophys. J.* **664** 680–686 (*Preprint arXiv:astro-ph/0701921*)
- [118] Cooray A R and Hu W 2000 *Astrophys. J.* **534** 533–550 (*Preprint astro-ph/9910397*)
- [119] Babich D and Pierpaoli E 2008 *Phys. Rev. D* **77** 123011 (*Preprint 0803.1161*)
- [120] Nishizawa A J, Komatsu E, Yoshida N, Takahashi R and Sugiyama N 2008 *Astrophys. J. Lett.* **676** L93–L96 (*Preprint 0711.1696*)
- [121] Nitta D, Komatsu E, Bartolo N, Matarrese S and Riotto A 2009 *Journal of Cosmology and Astro-Particle Physics* **5** 14–+ (*Preprint 0903.0894*)
- [122] Bartolo N, Matarrese S and Riotto A 2006 *JCAP* **0606** 024 (*Preprint astro-ph/0604416*)
- [123] Bartolo N, Matarrese S and Riotto A 2007 *JCAP* **0701** 019 (*Preprint astro-ph/0610110*)
- [124] Khatri R and Wandelt B D 2009 *Phys. Rev. D* **79**(2) 023501–+ (*Preprint 0810.4370*)
- [125] Khatri R and Wandelt B D 2009 *ArXiv e-prints, arXiv:0903.0871* (*Preprint 0903.0871*)
- [126] Senatore L, Tashev S and Zaldarriaga M 2009 *Journal of Cosmology and Astro-Particle Physics* **8** 31–+ (*Preprint 0812.3652*)

- [127] Senatore L, Tashev S and Zaldarriaga M 2009 *Journal of Cosmology and Astroparticle Physics* **9** 38–+ (Preprint 0812.3658)
- [128] Pitrou C 2009 *Classical and Quantum Gravity* **26**(6) 065006–+ (Preprint 0809.3036)
- [129] Pitrou C 2009 *General Relativity and Gravitation* **41** 2587–2595 (Preprint 0809.3245)
- [130] Pitrou C, Uzan J and Bernardeau F 2008 *Phys. Rev. D* **78**(6) 063526–+ (Preprint 0807.0341)
- [131] Pitrou C, Uzan J P and Bernardeau F 2010 (Preprint 1003.0481)
- [132] Beneke M and Fidler C 2010 (Preprint 1003.1834)
- [133] Spergel D N and Goldberg D M 1999 *Phys. Rev. D* **59** 103001
- [134] Bartolo N and Riotto A 2009 *JCAP* **0903** 017 (Preprint 0811.4584)
- [135] Starobinsky A A 1985 *JETP Lett.* **42** 152–155
- [136] Sasaki M and Stewart E D 1996 *Prog. Theor. Phys.* **95** 71–78
- [137] Creminelli P, Senatore L and Zaldarriaga M 2007 *Journal of Cosmology and Astroparticle Physics* **3** 19–+ (Preprint arXiv:astro-ph/0606001)
- [138] Sefusatti E 2009 *Phys. Rev.* **D80** 123002 (Preprint 0905.0717)
- [139] Giannantonio T and Porciani C 2009 (Preprint 0911.0017)
- [140] Bennett C L, Banday A J, Górski K M, Hinshaw G, Jackson P, Keegstra P, Kogut A, Smoot G F, Wilkinson D T and Wright E L 1996 *Astrophys. J. Lett.* **464** L1
- [141] Komatsu E, Wandelt B D, Spergel D N, Banday A J and Górski K M 2002 *Astrophys. J.* **566** 19–29
- [142] Komatsu E, Kogut A, Nolta M R, Bennett C L, Halpern M, Hinshaw G, Jarosik N, Limon M, Meyer S S, Page L, Spergel D N, Tucker G S, Verde L, Wollack E and Wright E L 2003 *Astrophys. J. Suppl.* **148** 119–134
- [143] Creminelli P, Senatore L, Zaldarriaga M and Tegmark M 2007 *JCAP* **0703** 005 (Preprint astro-ph/0610600)
- [144] Spergel D N, Bean R, Doré O, Nolta M R, Bennett C L, Dunkley J, Hinshaw G, Jarosik N, Komatsu E, Page L, Peiris H V, Verde L, Halpern M, Hill R S, Kogut A, Limon M, Meyer S S, Odegard N, Tucker G S, Weiland J L, Wollack E and Wright E L 2007 *Astrophys. J. Suppl.* **170** 377–408 (Preprint arXiv:astro-ph/0603449)
- [145] Yadav A P S and Wandelt B D 2008 *Physical Review Letters* **100**(18) 181301–+
- [146] Munshi D and Heavens A 2010 *Mon. Not. R. Astr. Soc.* **401** 2406–2418 (Preprint 0904.4478)
- [147] Smidt J, Amblard A, Serra P and Cooray A 2009 *Phys. Rev. D* **80**(12) 123005–+ (Preprint 0907.4051)
- [148] Jarosik N *et al.* 2010 *Astrophys. J. Suppl.*, submitted (Preprint 1001.4744)
- [149] Gold B *et al.* 2010 *Astrophys. J. Suppl.*, submitted (Preprint 1001.4555)

- [150] Bennett C L *et al.* 2010 *Astrophys. J. Suppl.*, submitted (*Preprint* 1001.4758)
- [151] Weiland J L *et al.* 2010 *Astrophys. J. Suppl.*, submitted (*Preprint* 1001.4731)
- [152] Cabella P, Pietrobon D, Veneziani M, Balbi A, Crittenden R, de Gasperis G, Quercellini C and Vittorio N 2009 *ArXiv e-prints* (*Preprint* 0910.4362)
- [153] Calabrese E, Smidt J, Amblard A, Cooray A, Melchiorri A, Serra P, Heavens A and Munshi D 2010 *Phys. Rev. D* **81**(4) 043529– (Preprint 0909.1837)
- [154] Munshi D, Valageas P, Cooray A and Heavens A 2009 *ArXiv e-prints*, *arXiv:0907.3229* (*Preprint* 0907.3229)
- [155] Kunz M, Banday A J, Castro P G, Ferreira P G and Górski K M 2001 *Astrophys. J. Lett.* **563** L99–L102
- [156] Munshi D, Heavens A, Cooray A, Smidt J, Coles P and Serra P 2009 *ArXiv e-prints*, *arXiv:0910.3693* (*Preprint* 0910.3693)
- [157] Gott J R I, Park C, Juszkiewicz R, Bies W E, Bennett D P, Bouchet F R and Stebbins A 1990 *Astrophys. J.* **352** 1–14
- [158] Mecke K R, Buchert T and Wagner H 1994 *Astr. & Astrophys.* **288** 697–704 (*Preprint* *arXiv:astro-ph/9312028*)
- [159] Schmalzing J and Buchert T 1997 *Astrophys. J. Lett.* **482** L1+ (*Preprint* *arXiv:astro-ph/9702130*)
- [160] Schmalzing J and Gorski K M 1998 *Mon. Not. R. Astr. Soc.* **297** 355–365
- [161] Winitzki S and Kosowsky A 1998 *New Astronomy* **3** 75–100
- [162] Hikage C, Komatsu E and Matsubara T 2006 *Astrophys. J.* **653** 11–26 (*Preprint* *arXiv:astro-ph/0607284*)
- [163] Matsubara T 2010 *Phys. Rev. D*, in press (*Preprint* 1001.2321)
- [164] Hikage C *et al.* 2008 *Mon. Not. Roy. Astron. Soc.* **389** 1439–1446 (*Preprint* 0802.3677)
- [165] Hikage C, Koyama K, Matsubara T, Takahashi T and Yamaguchi M 2009 *Mon. Not. Roy. Astron. Soc.* **398** 2188–2198 (*Preprint* 0812.3500)
- [166] Natoli P *et al.* 2009 *Mon. Not. R. Astron. Soc.*, submitted (*Preprint* 0905.4301)
- [167] Martínez-González E, Gallegos J E, Argueso F, Cayon L and Sanz J L 2002 *Mon. Not. Roy. Astron. Soc.* **336** 22 (*Preprint* *astro-ph/0111284*)
- [168] Martínez-González E 2008 *Proceedings of the IAC Winter School 2007, “Cosmic Microwave Background: from quantum fluctuations to the present universe”* (*Preprint* 0805.4157)
- [169] Curto A, Martínez-González E, Mukherjee P, Barreiro R B, Hansen F K, Liguori M and Matarrese S 2009 *Mon. Not. R. Astr. Soc.* **393** 615–622
- [170] Curto A, Martínez-González E and Barreiro R B 2009 *Astrophys. J.* **706** 399–403 (*Preprint* 0902.1523)
- [171] Mukherjee P and Wang Y 2004 *Astrophys. J.* **613** 51–60 (*Preprint* *arXiv:astro-ph/0402602*)

- [172] Cabella P *et al.* 2005 *Mon. Not. Roy. Astron. Soc.* **358** 684–692 (*Preprint* astro-ph/0406026)
- [173] Marinucci D, Pietrobon D, Balbi A, Baldi P, Cabella P, Kerkyacharian G, Natoli P, Picard D and Vittorio N 2008 *Mon. Not. R. Astr. Soc.* **383** 539–545 (*Preprint* 0707.0844)
- [174] Rudjord Ø, Groeneboom N E, Eriksen H K, Huey G, Górski K M and Jewell J B 2009 *Astrophys. J.* **692** 1669–1677 (*Preprint* 0809.4624)
- [175] Pietrobon D, Cabella P, Balbi A, de Gasperis G and Vittorio N 2009 *Mon. Not. R. Astr. Soc.* **396** 1682–1688 (*Preprint* 0812.2478)
- [176] Rudjord O *et al.* 2010 *Astrophys. J.* **708** 1321–1325 (*Preprint* 0906.3232)
- [177] Pietrobon D, Cabella P, Balbi A, Crittenden R, de Gasperis G and Vittorio N 2010 *Mon. Not. R. Astr. Soc.* **402** L34–L38 (*Preprint* 0905.3702)
- [178] Aghanim N, Kunz M, Castro P G and Forni O 2003 *Astron. Astrophys.* **406** 797–816 (*Preprint* astro-ph/0301220)
- [179] Jin J, Starck J, Donoho D L, Aghanim N and Forni O 2005 *Journal on Applied Signal Processing* **15** 2470–+ (*Preprint* arXiv:astro-ph/0503374)
- [180] Gaztañaga E and Wagg J 2003 *Phys. Rev. D* **68**(2) 021302–+
- [181] Chen G and Szapudi I 2005 *Astrophys. J.* **635** 743–749 (*Preprint* arXiv:astro-ph/0508316)
- [182] Cabella P, Hansen F K, Liguori M, Marinucci D, Matarrese S, Moscardini L and Vittorio N 2006 *Mon. Not. R. Astr. Soc.* **369** 819–824 (*Preprint* arXiv:astro-ph/0512112)
- [183] Chen G and Szapudi I 2006 *Astrophys. J. Lett.* **647** L87–L90 (*Preprint* arXiv:astro-ph/0606394)
- [184] Vielva P and Sanz J L 2009 *Mon. Not. R. Astr. Soc.* **397** 837–848
- [185] Baumann D *et al.* (CMBPol Study Team) 2009 *AIP Conf. Proc.* **1141** 10–120 (*Preprint* 0811.3919)